Policy Research Working Paper 10995

Impacts of Disasters in Conflict Settings

Evidence from Mozambique and Nigeria

Karima Ben Bih
Chloe Desjonqueres
Bramka Jarafino
Elodie Blanc
Solene Masson

WORLD BANK GROUP
Urban, Disaster Risk Management, Resilience and Land Global Department
December 2024

Policy Research Working Paper 10995

Abstract

This paper estimates the differentiated economic impact of natural hazard-related disasters (the specific disasters and climate shocks studied here being floods) when they occur in conflict versus non-conflict affected areas. Existing literature shows that disasters and climate shocks can cause significant distress to countries and people on an institutional and household level. However, assumptions are made that their impact tends to be larger in conflict-affected areas, with little evidence available on the differentiated extent of these damages. This paper investigates whether, and to what extent, the presence of conflicts has amplified the impacts of floods on economic activity and people, and hampered recovery. The paper applies a "top-down" approach to estimating the differential impacts of disasters and climate shocks between conflict and non-conflict affected areas using satellite-derived imagery of nightlight radiance as a proxy for economic activity, along with geospatial footprints of floods. The analysis considers two case studies: the 2019 tropical cyclones Idai and Kenneth and subsequent floods in Mozambique, and the July 2022 floods in Nigeria. Using difference-in-difference estimations, the analysis finds that there are significant differences in disaster and climate shock impacts and recovery between conflict and non-conflict affected areas. Particularly, there is a greater decline in economic activity and a longer recovery time in conflict affected areas, as proxied by the greater change in the intensity of nightlight radiance.

This paper is a product of the Urban, Disaster Risk Management, Resilience and Land Global Department. It is part of a larger effort by the World Bank to provide open access to its research and make a contribution to development policy discussions around the world. Policy Research Working Papers are also posted on the Web at http://www.worldbank.org/prwp. The authors may be contacted at kbenbih@worldbank.org.

Impacts of Disasters in Conflict Settings:
Evidence from Mozambique and Nigeria

Novembre 20, 2024

Karima Ben Bih, World Bank
Chloe Desjonqueres, World Bank
Bramka Jarafino, World Bank
Elodie Blanc, Motu Economic and Public Policy Research Center
Solene Masson, World Bank

Keywords: Economic Impacts of Disasters in Conflict, Climate shocks; Earth Observations; NPP-VIIRS; Floods; Nigeria; Mozambique; Conflicts influence on Disaster Impacts and Recovery;GDP.

JEL Classification: D74; O23 ; O47 ; O57 ; Q34; Q54 .

The authors are grateful to Stephane Hallegatte, Oscar Ishizawa, and Jun Rentschler for their thoughtful comments, suggestions, and guidance.

Introduction

The aim of this study is to examine the differential impact of disasters and climate shocks on populations in conflict-affected regions, specifically investigating the repercussions of flooding in conflict versus non-conflict areas. Using remote sensing technology, we attempt to overcome the challenge of data scarcity in conflict-affected countries, allowing us to account for short-term impacts of recent disaster and climate shock events. Despite the inherent limitations of using nightlight intensity as an economic activity indicator, it provides an empirical foundation for the analysis and enough observations for an ex-post quasi-experimental impact evaluation. We employ a difference-in-difference econometric approach, using satellite imagery of nightlight radiance alongside geospatial data on flood and conflict events. This methodological framework is applied to assess the aftermath of the March-April 2019 Floods in Mozambique following Cyclones Kenneth and Idai, as well as the 2022 floods spanning July to October in Nigeria.

Results show significant disparities in the effects of disasters and climate shocks between conflict-affected and non-conflict-affected areas. Specifically, we observe a more pronounced decline in economic activities in conflict-affected regions.

The paper is structured as follows. The first section outlines the context of flood and conflicts. It pays attention to the interconnectedness of conflict and disasters and climate shocks, outlining the methodology and empirical strategy derived to estimate such ex-post impact. In the second section, we present the results and supporting data derived from the study, including the case studies on Mozambique and Nigeria. Finally, we discuss limitations as well as broader implications before concluding.

Context: Flood impact and conflict affected population (Literature)

1. Impact of flood

Quantitative economic analyses have frequently used nightlight radiance as proxy for economic activity (Chen & Nordhaus, 2011; Henderson et al., 2012). These have also been used to estimate the impacts of weather variability and disasters and climate shocks (Bertinelli & Strobl, 2013; Elliott et al., 2015; Felbermayr et al., 2022; Heger & Neumayer, 2019; Miranda Montero et al., 2017) and, more specifically, floods (Kocornik-Mina et al., 2020). Most analyses using nightlight data usually demonstrate a negative impact of disaster and climate shocks on nightlights but with effects resorbing within the year following the event (Bertinelli & Strobl, 2013; Elliott et al., 2015; Gillespie et al., 2014). Schippers & Botzen (2023) find that for a severe disaster such as Hurricane Katrina, the effect can be longer lasting.

However, there is a debate about the accuracy of nightlights as a proxy for economic activity. Critics argue that nightlight intensity may not capture economic activity accurately in all contexts, such as highly rural areas, where changes in lighting efficiency could affect the amount of light observed without necessarily reflecting changes in economic activity. Possibly other cultural and social factors or government policies on lighting could also influence the amount of nightlight observed.

Despite these concerns, nightlights have several advantages as a data source. They are globally available, providing coverage even in regions where economic data might be scarce or unreliable. Nightlights also have a standard spatial resolution and time intervals, which allows for consistent comparisons over time and across different geographic areas. When processed and interpreted correctly, taking into account the potential limitations and biases, nightlight data can indeed serve as a useful proxy for the intensity of economic activity (Gibson et al., 2021).

2. Relationship between disaster and conflict-affected population

Explicit studies of the relationship between disaster and climate risk and conflict have gained traction over the past decade (Siddiqi, 2018), specifically focusing on co-location and causation debates associated with climate-related hazards, violent and armed conflict, and insecurity (Gemenne et al., 2014; Gleditsch, 2012). Often, previous studies have focused on the impacts of disasters on conflicts – whether they exacerbate existing conflicts, ignite new ones, or in some cases halt ongoing conflicts (Nel & Regharts, 2008; Schleussner et al., 2016; Slettebak, 2012; Ghimire et al., 2015; Nardulli et al., 2015). Due to such uncertain impacts of disasters and disaster recovery effort on conflicts, other studies explore how disaster risk reduction and recovery measures should be done differently in conflict contexts (Brzoska, 2018; Peters et al., 2019; World Bank, 2016).

Despite the growing body of literature related to the intricacies of disasters and conflicts, less attention has been given to understanding and quantifying the influences of conflicts on disaster impacts – the additional economic impacts of disasters should they take place in conflict areas and its effect on conflict-affected population – as well as the causal pathways and mechanisms behind such additional impacts. The absence of comprehensive economic data and ground truth data to validate disaster impacts, coupled with the complexity of defining conflict-affected populations are among the scientific challenges prohibiting analyzing the influence of conflicts on disaster impacts. This paper seeks to address this gap and support further quantitative analyses on the additional impact on households' welfare and nations' economic growth in countries experiencing these compounded crises.

Empirical strategy

Data

In this study, we use pixel-level geospatial data, including nightlights, flood footprints, population density, and administrative boundaries, to econometrically analyze the specific effects of flood events in Mozambique as well as Nigeria's conflict and non-conflict affected regions.

Nightlights data

Furthermore, we utilize composite images of nighttime radiance data captured by the Visible Infrared Imaging Radiometer Suite (VIIRS) sensor aboard the NASA-NOAA Suomi satellite. These monthly composites are available since 2012 at a resolution of 15 arcseconds by 15 arcseconds (approximately 463 meters at the equator). VIIRS Day Night Bands (DNB) data exclude grid cells affected by lightning, stray light, lunar illumination, and cloud cover (Elvidge et al., 2017). We favor VIIRS data over traditionally used data from the Defense Meteorological Satellite Program (DMSP)

due to several limitations identified in the latter, including blurring, lack of calibration, top-coding, and poor suitability as a GDP proxy in rural areas (Gibson et al., 2021).

To address challenges associated with using VIIRS nightlights data as a proxy for economic activity (Skoufias et al., 2021), we apply filters to remove pixels with extreme values (i.e., we restrict the sample to values comprised between the 1st and 99th percentiles) and account for the number of observations available per pixel.[1] We calculate the average nightlight radiance monthly spanning from 1 to 6 months before and after the occurrence of the 2019 floods in Mozambique and the 2022 floods in Nigeria. Two variables are computed: "avg_rad," representing the nightlight radiance at the flooded pixel level, and "avg_radBuff05" which averages for each flooded pixel the nightlight radiance of the pixel itself and adjacent pixels within a 0.5-kilometer buffer.[2] The latter variable is preferred to ensure maximum observation availability and to capture the impact on indirectly affected grid cells.[3] We also extracted the associated variables "cf_cvg" and "avg_cvgBuff05", which indicate the number of cloud-free observations in the month used to calculate average nightlight radiance.[4]

Flood data

Flood events are determined based on the methodology outlined by DeVries et al. (2020). We use S1 Ground Range Detected scenes from the Synthetic Aperture Radar sensors onboard the Sentinel-1 satellite, part of the European Space Agency's Copernicus program (ESA, 2023). These scenes provide data on Z-scores derived from SAR backscatter time series of single band co-polarization vertical transmit vertical receive (VV) and dual cross-polarization vertical transmit horizontal receive (VH). Since October 2014, this data has been available every 6 days at a 10-meter resolution.

Floods are defined as the unexpected presence of water observed in any given pixel. To distinguish floods from permanent or seasonally occurring surface water, we utilize the historical Landsat-derived monthly water probabilities dataset produced by the European Commission's Joint Research Centre (Pekel et al., 2016). Flood confidence is categorized as high if both VV and VH Z-scores fall below the identified thresholds, and as medium if only one of these polarizations is below the thresholds. We classify floods in areas not designated as permanent open water (with a probability of water greater than 95%) or with a historical inundation probability less than or equal to 25%. For each case study, we preselect a historical reference period based on existing knowledge of past flooding events in the respective area.

Conflict data

Conflict areas are identified utilizing geocoded data sourced from the Armed Conflict Location & Event Data Project (ACLED) database (ACLED, 2023), covering the period from January 2012 to December 2023 for Nigeria and from January 2016 to December 2023 in Mozambique. For the purpose of this study, conflict, as defined by the WBG (2024) is, "a state of acute insecurity resulting from the use of lethal force by a group— encompassing state forces, organized non-state entities, or other irregular bodies— driven by a political purpose or motivation. Such force may manifest

[1] Pixels with no cloud-free observations are excluded.
[2] A pixel is around 100m2, we tested without buffer, 500m and 1km and chose a 500m buffer to introduce more variation of nightlight intensity within flooded pixels.
[3] A time series depicting both variables is provided in Figure 16 in the appendices for Nigeria.
[4] The corresponding time series for is presented in Figure 17 for Nigeria.

bilaterally— involving engagements among multiple organized, armed factions, occasionally leading to collateral civilian harm— or unilaterally, wherein a group targets civilians deliberately." Furthermore, for the most precise depiction of areas severely affected by conflict, fatalities stemming from protests, riots, and strategic development (as per ACLED data) have been excluded, maintaining consistency with the WBG Classification of Fragility and Conflict Situation's (FCS) objectives and the scope of this study. Our analysis focuses on conflict records categorized as 'Battles', 'Explosions/Remote violence', and 'Violence against civilians'. These types of conflicts are selected due to their violent nature.

Settlement data

To determine the urbanization level, we use the Global Human Settlement Layer (GHSL) which combines gridded population data estimated by CIESIN GPW v4.11 GHS-POP R2023 and built-up surface information from Landsat and Sentinel-2 data GHS-BUILT-S R2023 (Schiavina et al., 2023).[5] The settlement data are available at the 1km resolution. We consider the data for the year 2020, which is the closest available to the time period of interest for both countries. In case of Nigeria, we defined 'urban' areas as cells defined as high-density cluster,[6] 'suburban' as moderate-density cluster,[7] 'rural' as rural and low-density clusters[8] and 'Uninhabited' as very low density rural and water covered areas (Figure 1).[9]

[5] In Google Earth Engine, this Image collection is accessible through https://developers.google.com/earth-engine/datasets/catalog/JRC_GHSL_P2023A_GHS_SMOD.

[6] The 'urban' category includes the classes 30: "Urban Centre grid cell", 23: "Dense Urban Cluster grid cell".

[7] The 'suburban' category includes the classes 22: "Semi-dense Urban Cluster grid cell" and 21: "Suburban or peri-urban grid cell".

[8] The 'rural' category includes the classes 13: "Rural cluster grid cell" and 12: "Low Density Rural grid cell".

[9] The 'uninhabited' category includes the classes 11: "Very low density rural grid cell" and 10: "Water grid cell".

Figure 1. Settlement categories in Nigeria

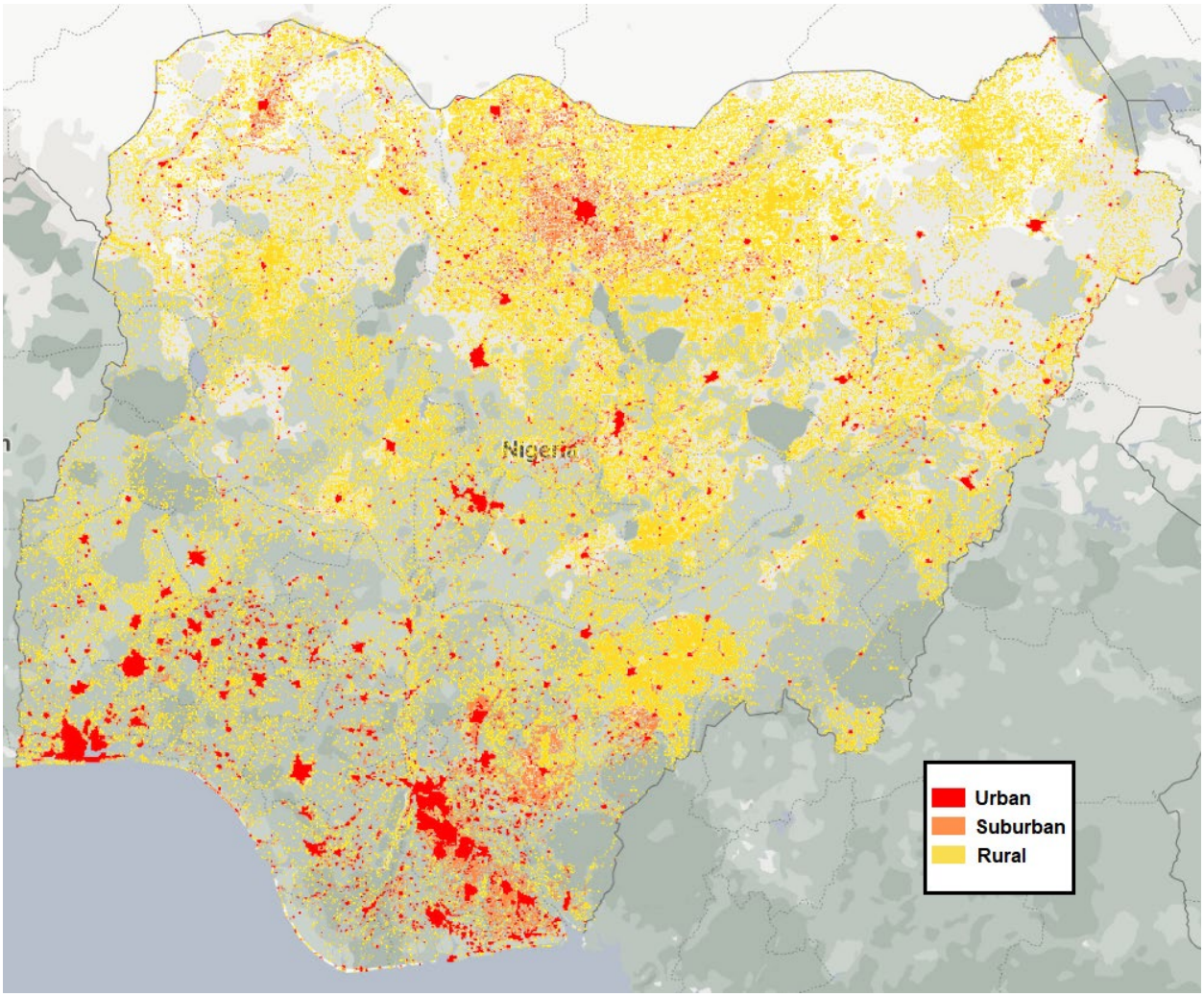

Population data

To maintain consistency with settlement data, population density estimates at the grid cell level are sourced from the High-Resolution Settlement Layer (HRSL) dataset *(Facebook Connectivity Lab and Center for International Earth Science Information Network - CIESIN - Columbia University., 2016)*. These data are available at a resolution of 1 arc-second (approximately 30 meters) for the year 2020. Additionally, alternative population data are extracted from the WorldPop database *(Linard et al., 2012; WorldPop.org, 2024),* available at a resolution of 100 meters for the year 2020.

Table 1 below describes the variables used in the analysis of flood and conflict impacts on economic activity, as measured by nightlight changes. The 'lat' (latitude) and 'lon' (longitude) variables allow for location mapping and situating the analysis spatially. The 'months_EE' variable aids in understanding the temporal effects of floods by indicating months after the event and negative values indicating the months preceding.

The 'flood' variable is crucial for assessing the impact of floods with varying degrees of data reliability. 'PopDens' provides insights into how population density might influence or be influenced by specific flood events. The variables 'cf_cvgBuff05' and 'avg_radBuff05' described above, measure economic activity through cloud observations and nightlight radiance, respectively. Additionally, they are averaged over adjacent pixels to provide context for each location.

'Treated' and 'Treated_after' distinguish areas affected by conflict before and after the flood in each country : March-April 2019 are months where the flood occurred in Mozambique while July 2022 was considered as the flooding month in this analysis for Nigeria. This is essential for determining the causal inference of conflict impact. 'Settlement' and 'Urban_Suburban' categorize urbanization levels to understand how different types of areas are affected by and respond to both floods and conflict events. Lastly, 'Fatalities' provides a direct measure of the human cost of conflicts.

These variables collectively enable a comprehensive analysis of the effects of floods and conflicts when they co-occur in the same location. They are used to analyze the impacts of floods and conflict on specific aspects of economic activity, as potentially inferred by nightlight changes. Table 1 describes these variables, their units of measurements, and how they will be used in the analysis.

Table 1. Description of variables

Variables	Description	Unit
lat	latitude	Decimal coordinates
lon	longitude	Decimal coordinates
months_EE	Month since the event	Months (positive if after event, negative if before event)
flood	Flood variable	=1 or 2 if medium reliability, =3 if high reliability
PopDens	HRSL population density	Person/km^2
cf_cvgBuff05	Total number of cloud-free observations that went into each pixel (averaged over the adjacent pixels)	
avg_radBuff05	Average nightlight radiance values (averaged over the adjacent pixels)	nanoWatts/sr/cm^2
Treated	Dummy variable representing conflict-affected area	=1 if subject to a conflict within the buffer area before the floods, =0 otherwise
Treated_after	Dummy variable representing conflict-affected area	=1 if subject to a conflict within the buffer area after the floods, =0 otherwise
settlement	Degree of Urbanization	=11 if uninhabited, =12 if rural, =21 if suburban and =23 if urban
Urban_Suburban	Urbanization dummy variable	=1 if urban or suburban, =0 otherwise
Fatalities	Total number of fatalities associated with conflicts within the buffer area	

Overall empirical strategy

To differentiate the impact of floods on economic activity prior to the flood between conflict-affected (treatment group), and non-conflict affected (control group) areas, we first restrict the sample to flood-impacted pixels. We then apply the difference-in-differences regression method, a quasi-experimental technique commonly used for ex-post impact evaluations. The underlying concept

involves comparing two groups over time. Due to their distinct characteristics, we expect differences in outcomes between the groups. However, the evolution of these differing outcomes over time, while holding group characteristics constant, should follow a similar trend (i.e., the common trend assumption) until an exogenous shock occurs. The presence of this parallel trend is crucial for establishing causal evidence of impact. The difference-in-differences research design is particularly suitable for 'event' studies and the quantification of the impact of unexpected shocks on economic outcomes. This method has been extensively employed in the reviewed literature (Card & Krueger, 2000; Galiani et al., 2005). In our case studies, we are using the canonical difference in difference, which means two groups and two time periods (before and after).

The difference-in-difference regression is specified as follows:

$$Y_{i,t} = Treated_i\beta_1 + \ Post\ Period_t\beta_2 + \ \text{Treatment}_{i,t}\beta_3 \ + covariates_{i,t}\beta_4 + \varepsilon_{it} \qquad (1)$$

where $Y_{i,t}$ is the average log of nightlights data for each flooded pixel *i* at time *t*. The use of remote sensing data allows us to explore immediate to short term impact of the flood over our two groups. $Treated_i$ is a dummy variable equal to 1 for flooded pixel *i* located within the conflict buffer zone before the flood event, and to 0 for flooded pixel *i* located in a non-conflict affected area before the flood event. $Post\ Period_t$ is a dummy variable that represents the period after the exogeneous shock.[10] $Treatment_{it}$ is the treatment variable, i.e., the variable of interest in a difference-in-difference specification which accounts for the interaction of the treated and Post period variable; $covariates_{it}$ is the set of additional explanatory variable suspected to impact the level of nightlights radiance; and ε_{it} is an independent and identically distributed error term, clustered at the administrative level 2, to avoid spatial autocorrelation.

One of the challenges in our analysis is the definition of conflict-affected areas. Conflict events in Mozambique are clustered geographically as such that it is readily ascertainable what regions are most impacted by these events, and thus defined as conflict-affected areas for the purpose of this study.

Due to the complexity and wide geographical span of violent and non-violent conflict events in Nigeria, conflict-affected areas in Nigeria are not defined based on number of events alone but are based on the WBG FCS conflict classification. This classification uses publicly available data to annually assess countries, pinpointing those most affected by fragility and conflict. This method differentiates between territories experiencing *Fragility* and/or *Conflict* situations. Aligned with this definition, the study employs the following conflict indicators identified by the FCS index to delineate conflict-affected areas in Nigeria at the Local Government Area (LGA) scale:

[10] This variable takes a value of 1 if *t* = August 2020 to estimate the effect 1 month after the disaster, *t* = November 2020 for the effect 3 months after the disaster, etc. and 0 otherwise.

(1) For ongoing conflict according to ACLED, (a) an absolute number of conflict deaths above 250, and (b) above 2 deaths per 100,000 population.
(2) For rapidly declining security situations according to ACLED, (a) an absolute number of conflict deaths above 250, (b) between 1 and 2 deaths per 100,000 population, and (c) the number of casualties has more than doubled in the past year.

Difference in difference methodology relies on different assumptions where the common trend is the most important one. To validate this assumption of common trends before the flood, indicating that the dependent variable for both groups would have continued moving similarly in the absence of the extreme event, we conduct a test by comparing changes in the dependent variable for the treatment and control groups over multiple periods preceding the floods (i.e. estimate the difference-in-difference between t-2 and t-1, the t-3 and t-2, etc.). This analysis helps ascertain whether the economic trajectories of the two groups were indeed parallel before the occurrence of the flood events. The regression is specified as:

$$Y_{i,t} = Treated_i\beta_1 + Post\ Period_t\beta_2 + \text{Treatment}_{i,t}\beta_3 + covariates_{i,t}\beta_4 + \varepsilon_{it} \qquad (2)$$

Variables are the same as specification (1) but the period of interest is not the same. We provide statistical tests as well as the common trend visually represented for each of our case study.

Case study selection

The study's focus on disaster impacts in conflict vs non conflict affected areas limits the pool of country case studies. There are several aspects that determine the choice of the case study countries. First, the selected countries need to have geographically localized conflicts, allowing for a controlled comparison where conflict is the primary differing factor of disaster impacts. Second, there is a requirement that the selected countries were affected by a rapid onset disaster in recent years, to increase the possibility of available data in assessing the disaster's impacts. If multiple countries are selected, the rapid-onset disaster events had to happen within the same time frame. This criterion ensures that the case studies provide a focused examination of the impact of disasters on economic activities in conflict setting vs non conflict settings, without the confounding effects of different country conditions or timelines of disaster events. Third, the disaster footprints should cover a substantial geographical extent of the selected countries' area as opposed to localized disasters. This criterion is to ensure that there are both conflict- and non-conflict-affected areas hit by the disaster. Given the criteria above, we selected the 2019 Tropical Cyclones Idai and Kenneth in Mozambique and the July 2022 floods in Nigeria as case studies. Furthermore, the two countries have comparable contexts in terms of conflict characteristics which are crucial for isolating the variable of conflict in comparative analysis.

Mozambique case study: 2019 Tropical Cyclones Idai and Kenneth

The first case study focuses on the floods in Mozambique after TC Idai and Kenneth. In 2019, Mozambique was hit by two Tropical Cyclones (TC), Idai (March 4-15) and Kenneth (April 25-28), both of which have been qualified as among the strongest TCs on record in the Southern Hemisphere (Charrua et al., 2021). The northeastern region of the country is characterized by a widespread long-

term humanitarian situation due to the ongoing conflict, dating back to 2017. As depicted in Figure 2, TC Idai first made landfall on March 4, 2019, until March 9, before changing direction and making a second landfall on March 14, this time close to the city of Beira in Central Mozambique. A month later, on April 25, TC Kenneth made landfall in the Cabo Delgado province. Subsequent flooding significantly impacted large areas of the country, affecting conflict- and non-conflict affected areas (see Figure 3 and Figure 4).

Figure 2. Tracks of TC Idai and TC Kenneth, Mozambique, 2019

Source: IBTrACS, 2019

Figure 3. Flood footprint following TC Idai

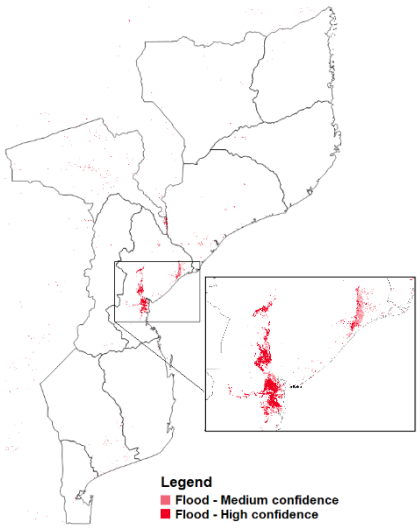

Figure 4. Flood footprint following TC Kenneth

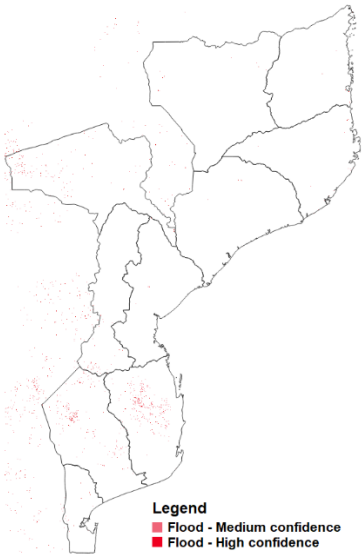

Source: Authors' elaboration using Google Earth Engine following DeVries et al. (2020)'s methodology.
Note: Flood extent is estimated over a week following each event, i.e from March 4 to 22, 2019 for TC Idai and April 25 to May 2, 2019 for TC Kenneth.

Table 2. Buffer size by settlement type for Mozambique

		Settlement type		
		Urban	Suburban	rural
Buffer size	Large	20km	40km	80km
	Small	10km	30km	60km

Descriptive statistics

Across all months (from September 2018 to October 2019) and flooded grid cells,[11] the unrestricted sample size is 5,755,486 observations (see Table 3). However, 94% of the sample pertains to

[11] We are accounting here pixels that have been flooded during the Kenneth and Idai cyclones in April and March 2019, respectively.

'uninhabited' grid cells, and only 1% is classified as 'Urban'. Following Skoufias et al. (2021) paper, 'Uninhabited' grid cells are removed from the estimation sample. Corresponding summary statistics are presented in Table 4 and Table 5. The size of the restricted sample is now of 427,553 pixels.

Table 3. Number of observations for the whole sample before selection

	settlement			
	Uninhabited	**Rural**	**Urban**	**Total**
Total Observations	5,410,141	303,450	41,895	5,755,486
Percentage of total	94%	5%	1%	

Table 4 presents a summary statistic based on the analysis of rural and urban flooded pixels. Notably, our main variable of interest, nightlights, exhibits a relatively low average intensity at the pixel level. This observation is aligned with the overall low density of distribution of nightlights, as corroborated by a population density of 16 person per km^2. Additionally, the average value of the urban dummy variable, which is close to 0, indicates a prevalence of rural flooded pixels over urban flooded pixels within our sample.

Table 4. Summary statistics for habited flooded pixels (rural and urban categories) sample

	N	**Mean**	**SD**	**Min**	**p5**	**Median**	**p95**	**Max**
PopDens	427,553	16.99	75.32	0	0	0	89.89	1367.76
cf_cvgBuff05	427,553	11.74	3.33	1	5.34	12	16.49	21
avg_radBuff05	427,553	1.02	4.16	0	0.06	0.2	3.75	88.18
urban	427,553	0.12	0.32	0	0	0	1	1

When considering the conflict-affected areas variable, the number of treated pixels – reflecting conflict-associated with each flooded grid cell - will depend on the conflict definition and buffer size considered. Table 5 provides a summary statistic of the number of conflicts and fatalities across different buffer sizes going from 10km to 100km.

Table 5. Summary statistics of variables differing by buffer size

Buffer size	**Variable**	**Mean**	**SD**	**Min**	**p5**	**Median**	**p95**	**Max**
100km	conflicts	16.71	59.46	0	0	5	45	740
	fatalities	4.12	11.59	0	0	1	14	156
90km	conflicts	13.98	49.77	0	0	4	38	645
	fatalities	3.54	10.15	0	0	1	12	154
80km	conflicts	11.56	41.84	0	0	4	31	577
	fatalities	3.03	9.19	0	0	1	11	135
70km	conflicts	9.25	34.58	0	0	2	26	526
	fatalities	2.48	7.93	0	0	0	10	113
60km	conflicts	7.15	27.23	0	0	1	25	422
	fatalities	1.98	6.82	0	0	0	9	102

50km	conflicts	5.69	21.33	0	0	1	22	371
	fatalities	1.64	5.68	0	0	0	9	95
40km	conflict	4.15	14.36	0	0	0	16	248
	fatalities	1.25	4.36	0	0	0	9	69
30km	conflicts	2.92	10.07	0	0	0	13	163
	fatalities	0.91	3.21	0	0	0	9	44
20km	conflicts	1.76	6.49	0	0	0	10	89
	fatalities	0.2	1.19	0	0	0	1	26
10km	conflicts	0.75	3.37	0	0	0	4	60
	fatalities	0.2	1.19	0	0	0	1	26

Number of observations: 427,553

In analyzing the spatial distribution of conflicts in Mozambique, we note in Figure 5 the average density of conflict events spanning from 2016 to 2023. It is worth noting that some regions exhibit higher density of conflict, namely Cabo Delgado, Sofala and Gaza. It is particularly striking to note the occurrence of over 500 incidents in each of these three states over the studied period, which denotes a concentration of conflicts in these regions. To provide a comprehensive analysis our investigation is expanded to include the prevalence of conflict spanning the designated period (2016-2023). This is visually depicted in Figures 5, 6, and 7. It is worth noting that the frequency of conflicts across all studied categories remained subdued prior to 2018. However, there was a significant surge in violence beginning in 2018, culminating in a peak in 2020 for incidents of violence against civilians, and in 2021 for battle-related conflicts. Even if we can observe a peak in the number of conflicts in 2018, we would rather use conflicts over a long-term period (meaning a few years before the floods). In doing so, we are dealing with treated areas that have been affected by a conflict over the long term and do not include flooded areas that might have been affected by a conflict a few years before the flood occurred. In the same way, all flooded pixels affected by a conflict after the cutoff date (March-April 2019) are not accounted in this analysis. We thus exclude them from our sample in order to avoid reverse causality: the flood reinforcing the number of conflicts.

Figure 5: Number of conflicts per regions in Mozambique, period 2016 to 2023.

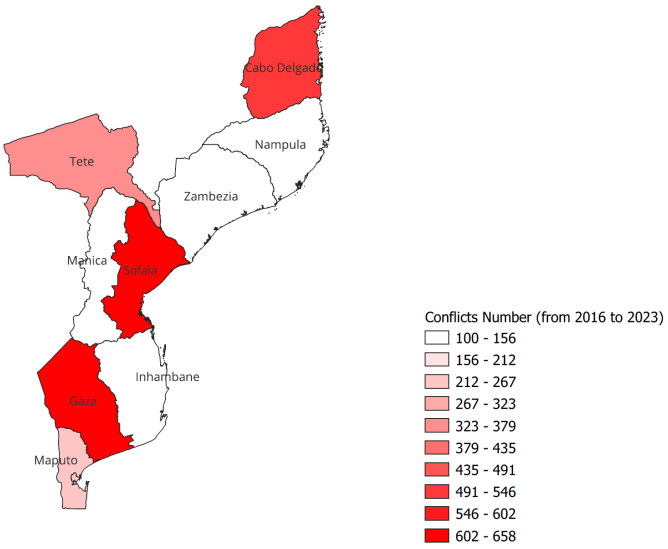

Source: authors' elaboration using ACLED data

Figure 6: Total number of conflicts in Mozambique, period 2016 to 2023.

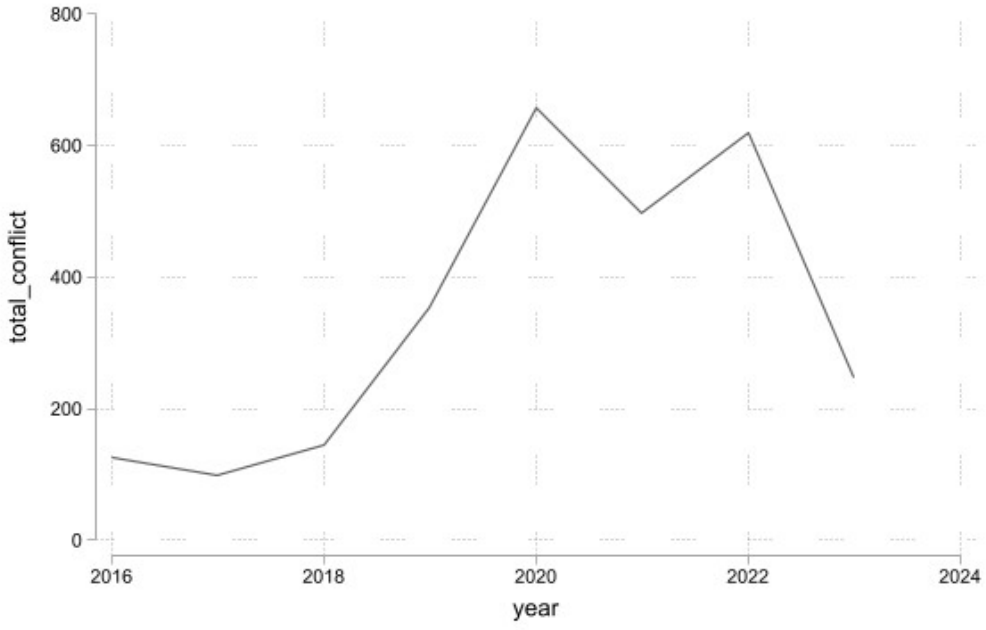

Source: authors' elaboration using ACLED data

Figure 7: Number of conflicts in Mozambique, period 2016 to 2023, by conflict types.

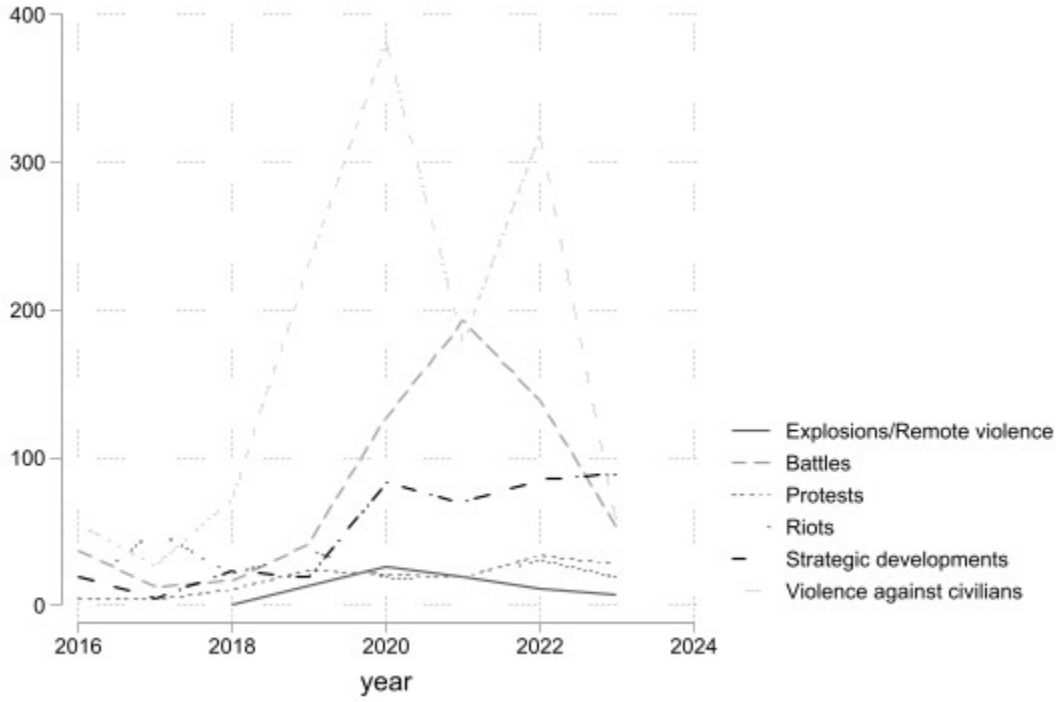

Source: ACLED data

As noted earlier in the text, the distribution of observations in the treatment and control groups is affected by the buffer zone (Table 5). As the buffer zone expands, there is a proportional increase in the treatment group and a decrease in the control group. Optimal balanced between the groups is obtained with a 60km buffer area around conflicts. As such, we have selected 60km buffer zone as the basis for our analysis. Results from the other buffer zone will be provided in the appendices to support sensitivity analysis.

Results: Mozambique

To estimate the difference-in-difference regression presented in equation (1) for Mozambique, we consider $Y_{i,t}$, the average log of nightlights data for each flooded pixel *i* at time *t*, with *t* ranging from 6 months prior the TC's induced floods (September 2018 to February 2019) and 6 months after (May 2019 to October 2019). Results are presented in Table 6 considering *avg_radBuff05* as the dependent variable. The variable of interest *did_var* (*Treated*PostPeriod),* estimating the differentiated impact of the cyclones on nightlights intensity one month after the TCs compared to one month before, is negative and significant. It reveals with high confidence that conflict-affected areas experienced a decline in economic activity that was 1.4 percent larger than non-conflict-affected areas one month after the cyclone hit.

Four different model specifications, using different covariates and control variables, were tested to check the consistency of the results (columns (1) to (4) in Table 6). As a first covariate, we included

pop_HRSL_dens_km2 to control for variations in population density across studied pixels, which could affect nightlights independently from disaster-induced changes in access to electricity. The second column of Table 6 includes the number of cloud-free observations that went into each pixel averaged over the adjacent pixels. This variable is insignificant, confirming that the nightlight radiance is not impacted by the quality of observations as represented by the number of observations that were used to calculate the monthly average values. The third column includes the urban dummy variable which is positive and significant reassuringly proving that nightlight is stronger in urban areas that in rural areas.[12] The last column includes the number of fatalities. This variable is not significant, indicating that the effect is not associated with the number of deaths related to the conflicts within the buffer zone.

Table 6. Regression results of equation (1) for conflicts within 60km buffer for 1 month post TCs. Dependent variable avg_radBuff05

	(1)	(2)	(3)	(4)
	Period -1 to 1	Period -1 to 1	Period -1 to 1	Period -1 to 1
VARIABLES	avg_radBuff05	avg_radBuff05	avg_radBuff05	avg_radBuff05
tot_treated	0.0291**	0.0297**	0.0197**	0.0175*
	(0.0113)	(0.0117)	(0.00990)	(0.0100)
temp_shock	-0.0366***	-0.0417***	-0.0366***	-0.0366***
	(0.00538)	(0.00934)	(0.00538)	(0.00538)
did_var	**-0.0134***	**-0.0149***	**-0.0134***	**-0.0134***
	(0.00795)	**(0.00889)**	**(0.00795)**	**(0.00795)**
pop_HRSL_dens_km2	0.00635***	0.00635***	0.00511***	0.00511***
	(0.000848)	(0.000848)	(0.000770)	(0.000770)
cf_cvgBuff05		0.00124		
		(0.00199)		
Urban			0.384***	0.384***
			(0.0642)	(0.0641)
tot_fatalities				0.00108
				(0.00102)
Constant	0.199***	0.186***	0.176***	0.174***
	(0.0131)	(0.0261)	(0.0114)	(0.0117)
Observations	16,880	16,880	16,880	16,880
R-squared	0.773	0.773	0.806	0.806
Treatment Obs	9684	9684	9684	9684
Control Obs	7196	7196	7196	7196

Notes: Robust standard errors in parentheses; *** p<0.01, ** p<0.05, * p<0.1; avg_radBuff05 ranges from 1st to 99th percentile (.02 to 21.8 nanoWatts/sr/cm^2)

[12] We also estimated this specification including interactions with the urban dummy variable to see if we would obtain different impacts for urban areas, but did not find a significant impact.

As depicted in Figure 8,[13] we observe a decline in economic activity in both conflict-affected and non-conflict affected areas between the dotted lines representing the landfall of Idai (left, in March 2019) and Kenneth (right, in April 2019). However, the decline is greater in conflict-affected areas, as evidenced by the slope of the red curve. Both groups experience further decline two months post TCs.

Figure 8. Time series of mean nightlight (avg_radBuff05) over months before and after Cyclone Idai and Kenneth in Mozambique using large conflict buffers. T=0 refers to March/April 2019.

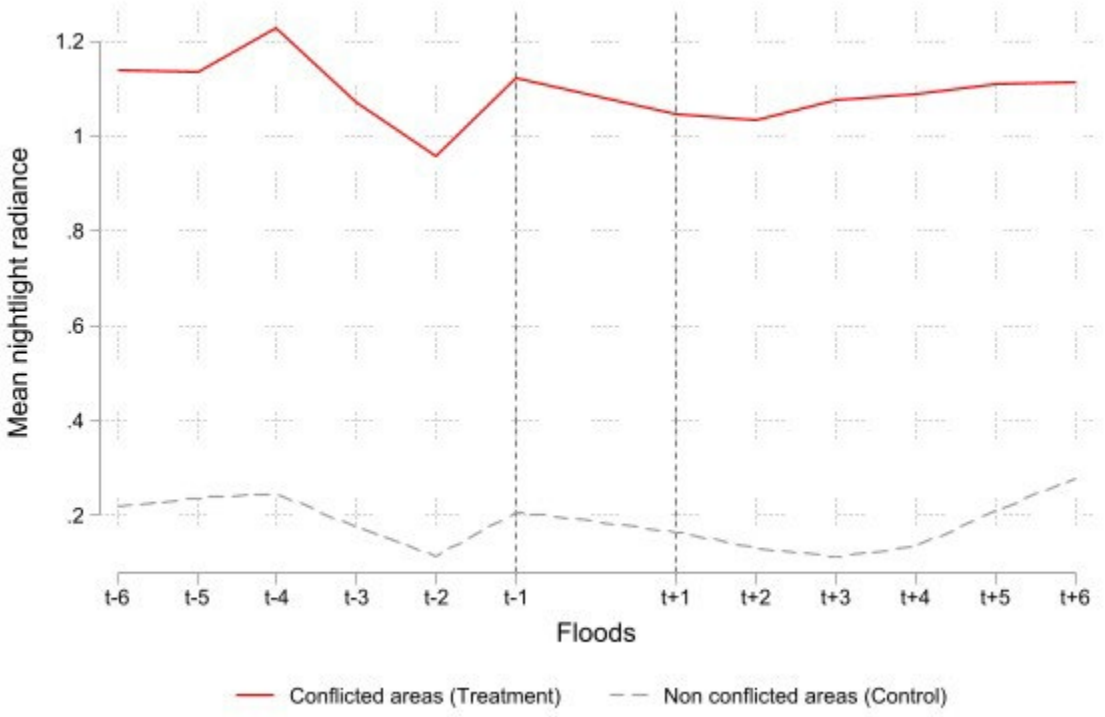

To assess the differential impacts of floods over a longer time period, we re-estimate the preferred specification considering the difference between the month before the TCs and 2 to 18 months after the event. Results for 1 to 6 months are presented in Table 7.

Based on results shown in Table 7 below and Figure 8 above, several significant patterns emerge across different time intervals following this disaster. In the immediate aftermath (*t+1*), there is a notable surge in impacts observed in conflict areas. The larger impacts in conflict areas could be attributed to the inherently lower quality of structures and infrastructure in these regions. Consequently, when confronted with disasters, the diminished resilience of conflict-affected areas results in a more pronounced reduction in nightlight radiance. Moving forward to *t+2, t+3, and t+4*, both conflict and non-conflict areas exhibit no statistically significant differences in their recovery, indicating a potential delay in the initiation of rehabilitation and reconstruction efforts across the board, or an equal access to resources (humanitarian aid, savings, etc.). However, by *t+5* and *t+6*, while non-conflict areas show signs of recovery, conflict areas continue to lag behind. This disparity

[13] The nightlights sample for conflict-affected areas presents more radiance than non-conflict-affected areas due to sample bias: conflict-affected areas are closer to urban areas than non-conflict affected areas.

in recovery rates suggests that in the medium term (*t+5* and *t+6*) non-conflict areas benefit from greater access to resources, institutional capacity, and potentially further financial support, facilitating their recovery process compared to conflict-affected regions.

Table 7. Regression results for conflicts within 60km buffer, preferred specification at different periods post TCs

	(1) Period -1 to 1	(2) Period -1 to 2	(3) Period -1 to 3	(4) Period -1 to 4	(5) Period -1 to 5	(6) Period -1 to 6
VARIABLES	avg_radBuff05	avg_radBuff05	avg_radBuff05	avg_radBuff05	avg_radBuff05	avg_radBuff05
tot_treated	0.0291**	0.0250**	0.0228**	0.0220**	0.0276***	0.0337***
	(0.0113)	(0.00998)	(0.0111)	(0.0109)	(0.0106)	(0.0105)
temp_shock	-0.0366***	-0.0683***	-0.0860***	-0.0653***	0.00238	0.0618***
	(0.00538)	(0.00422)	(0.00373)	(0.00535)	(0.00460)	(0.00503)
did_var	-0.0134*	0.000594	0.00802	0.00634	-0.00966*	-0.0142*
	(0.00795)	(0.00560)	(0.00705)	(0.00699)	(0.00499)	(0.00758)
pop_HRSL_dens_km2	0.00635***	0.00643***	0.00652***	0.00640***	0.00628***	0.00601***
	(0.000848)	(0.000863)	(0.000896)	(0.000895)	(0.000876)	(0.000830)
Constant	0.199***	0.200***	0.200***	0.202***	0.200***	0.201***
	(0.0131)	(0.0128)	(0.0134)	(0.0134)	(0.0131)	(0.0126)
Observations	16,880	16,880	16,880	16,880	16,880	16,880
R-squared	0.773	0.773	0.774	0.772	0.773	0.770
Treatment Obs	9684	9684	9684	9684	9684	9684
Control Obs	7196	7196	7196	7196	7196	7196

Notes: Robust standard errors in parentheses; *** p<0.01, ** p<0.05, * p<0.1; avg_radBuff05 ranges from 1st to 99th percentile (0.02 to 2.7 nanoWatts/sr/cm^2)

Robustness checks

We also ran the regression using only time periods prior to the disaster, from 6 to 1 months before the cyclones hit, to ensure that there were no significant pre-disaster nightlight variation discrepancies between the two groups that could have explained our results. The results presented in Table 8 and confirm that the *did_var* (*Treated*PostPeriod)* variable is not significant. This test implies that our findings are robust, and that usual nightlights variations do not drive the results of our difference-in-difference specification, confirming causality.

Table 8. Regression results for conflicts within 60km buffer testing common trends using log(nightlights), 1 to 6 months before the Tropical Cyclones

	(1) Period -2 to -1 Mozambique	(2) Period -3 to -2 Mozambique	(3) Period -4 to -3 Mozambique	(4) Period -5 to -4 Mozambique	(5) Period -6 to -5 Mozambique
VARIABLES	avg_radBuff05	avg_radBuff05	avg_radBuff05	avg_radBuff05	avg_radBuff05

tot_treated	0.0271***	0.0209**	0.0269***	0.0246**	0.0265***
	(0.00997)	(0.00939)	(0.00958)	(0.00995)	(0.00981)
temp_shock	0.0799***	-0.0529***	-0.0589***	0.00812**	0.0168***
	(0.00270)	(0.00394)	(0.00260)	(0.00318)	(0.00514)
did_var	-0.00383	0.00280	-0.00476	0.00122	-0.00428
	(0.00570)	(0.00482)	(0.00411)	(0.00545)	(0.00687)
pop_HRSL_dens_km 2	0.00639***	0.00648***	0.00646***	0.00634***	0.00629***
	(0.000899)	(0.000926)	(0.000887)	(0.000863)	(0.000860)
Constant	0.122***	0.175***	0.234***	0.228***	0.213***
	(0.0129)	(0.0129)	(0.0128)	(0.0126)	(0.0128)
Observations	16,880	16,880	16,880	16,880	16,880
R-squared	0.772	0.772	0.775	0.764	0.759
Treatment Obs	9684	9684	9684	9684	9684
Control Obs	7196	7196	7196	7196	7196

Notes: Robust standard errors in parentheses; *** p<0.01, ** p<0.05, * p<0.1; avg_radBuff05 ranges from 1st to 99th percentile (0.02 to 2.7 nanoWatts/sr/cm^2)

Nigeria case study: July 2022 floods

2022 flood event

According to EM-DAT & CRED / UCLouvain (2023), Nigeria suffered flooding during the period of July 1, 2022 to October 31, 2022. The first row of Figure 9 presents the flooded pixel during each month and over the whole period, The second row shows flooded pixel during each month but not flooded during the other months. During the first couple of months of the flooding season, most flooded pixels are located in the south. During the second part of the period, the floods mainly occur along the Benue and Niger Rivers in the center part of the country. Given the length of the flooding period and the potential for adaptation and population displacement after the first flooding events, we focus on the 'unexpected' first floods. Therefore, we select the pixels that were flooded in July but not in August, September or October.

Figure 9. Flooded pixel during each month and over the whole period (first row) and flooded pixel during each month but not flooded during the other months (second row)

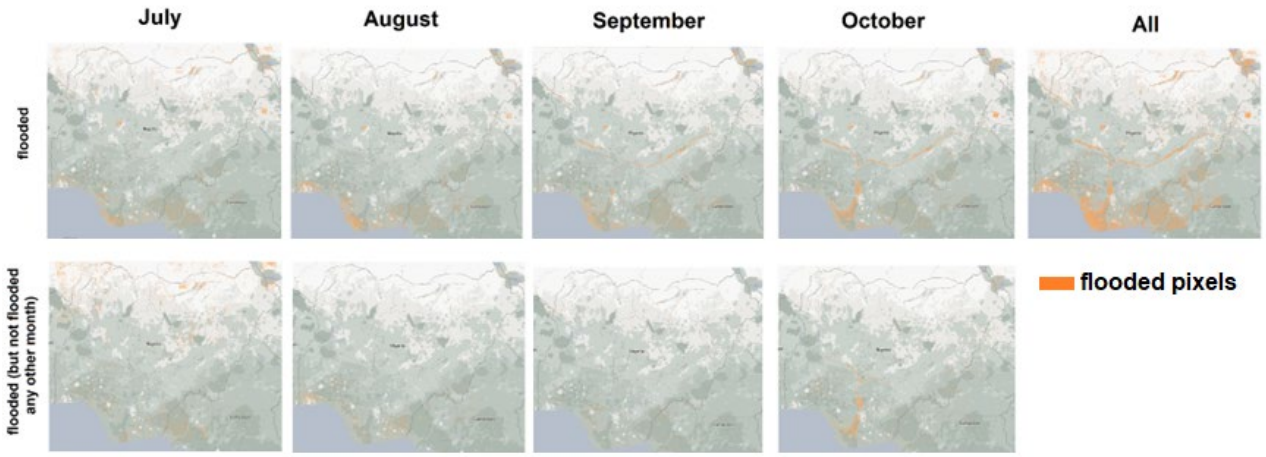

Descriptive statistics A description of the variables included in the dataset is provided in Table 1 in the empirical strategy section. Across all months and grid cells, the unrestricted sample size is 5,755,486 (see Table 9). While floods have caused serious damage and displacement over the period of July to October 2022 and beyond, in the confined time period used for the study (June 30th to July 30th, 2022) the affected territory is limited. During this period, 75% of the sample pertains to 'uninhabited' pixels, and 5% are 'Uninhabited' grid cells are removed from the estimation sample pixels.

Table 9. Number of observations for the whole sample before selection

	avg_radBuff05		**avg_rad**	
	Observations	Percentage of Total	Observations	Percentage of Total
Uninhabited	339,269	75%	335,733	75%
Rural	73,174	16%	72,525	16%
Suburban	42,399	9%	41,764	9%
Urban	21,955	5%	21,635	5%
All	454,842		450,022	

Table 10 provides information regarding statistics of variables included within our model. As in Mozambique, nightlights density in Nigeria is rather low (1.44), even though we can observe a higher density of population especially within urban areas. Indeed, in the case of Nigeria, we see that 5% of flooded pixels are within urban areas against 1% in Mozambique.

Table 10. Summary statistics for habited flooded pixels (rural, suburban and urban categories) sample for large conflict buffers

	N	Mean	SD	Min	p5	Median	p95	Max
PopDens	115,573	53.24	148.32	0	0	0	275.84	3,280.39
pop_WorldPop_dens_km2	115,573	42.54	118.59	0	2.18	14.87	160.69	3,977.57
cf_cvgBuff05	115,573	8.05	4.19	1	1.34	8.05	14	23.63
cf_cvg	114,340	8.13	4.17	1	2	8	14	24
avg_radBuff05	115,573	1.44	14	0	0.19	0.37	3.94	1,553.18
avg_rad	114,289	1.42	17.37	0.01	0.18	0.37	3.9	,2363.48
nb_conflict	115,573	4.1	14.19	0	0	0	18	625
Treated	115,573	0.39	0.49	0	0	0	1	1
Treated_after	115,573	0.22	0.41	0	0	0	1	1
Fatalities	115,573	19.37	137.01	0	0	0	49	4450
settlement	115,573	15.68	4.87	12	12	12	23	23
Urban_Suburban	115,573	0.37	0.48	0	0	0	1	1

The spatial distribution of conflict in figures 10, 11 and 12 below illustrates a pattern: the conflicts are uniformly distributed across Nigeria. The country has a broader spatial and temporal span of conflicts. Furthermore, the conflict intensity and spread are higher throughout the country, as opposed to Mozambique, which has a concentration of conflict in three states.

Figure 10. Number of conflicts in Nigeria at region level from 2011 to 2023.

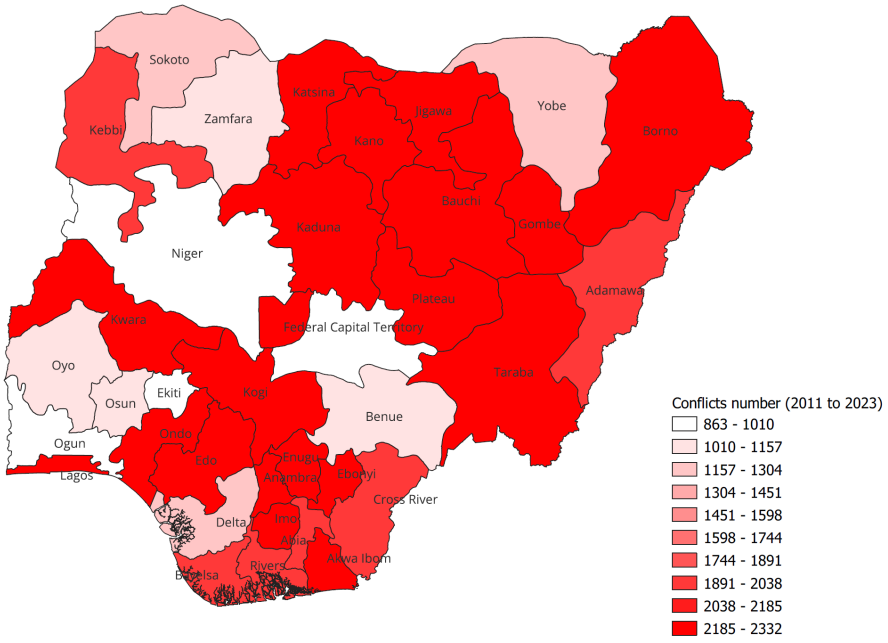

Source: ACLED data

Figure 11. Total number of conflicts in Nigeria from 2011 to 2023

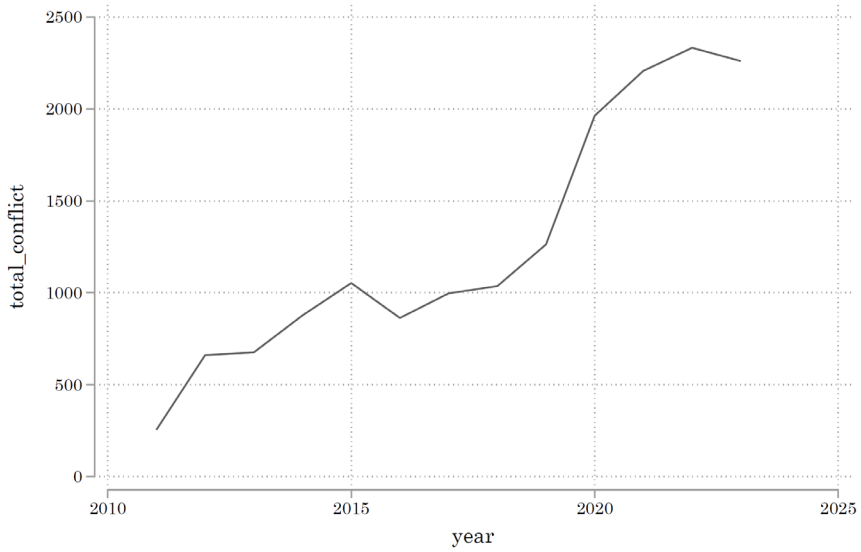

Source : ACLED data

Figure 12. Number of conflicts in Nigeria from 2011 to 2023, by conflict type.

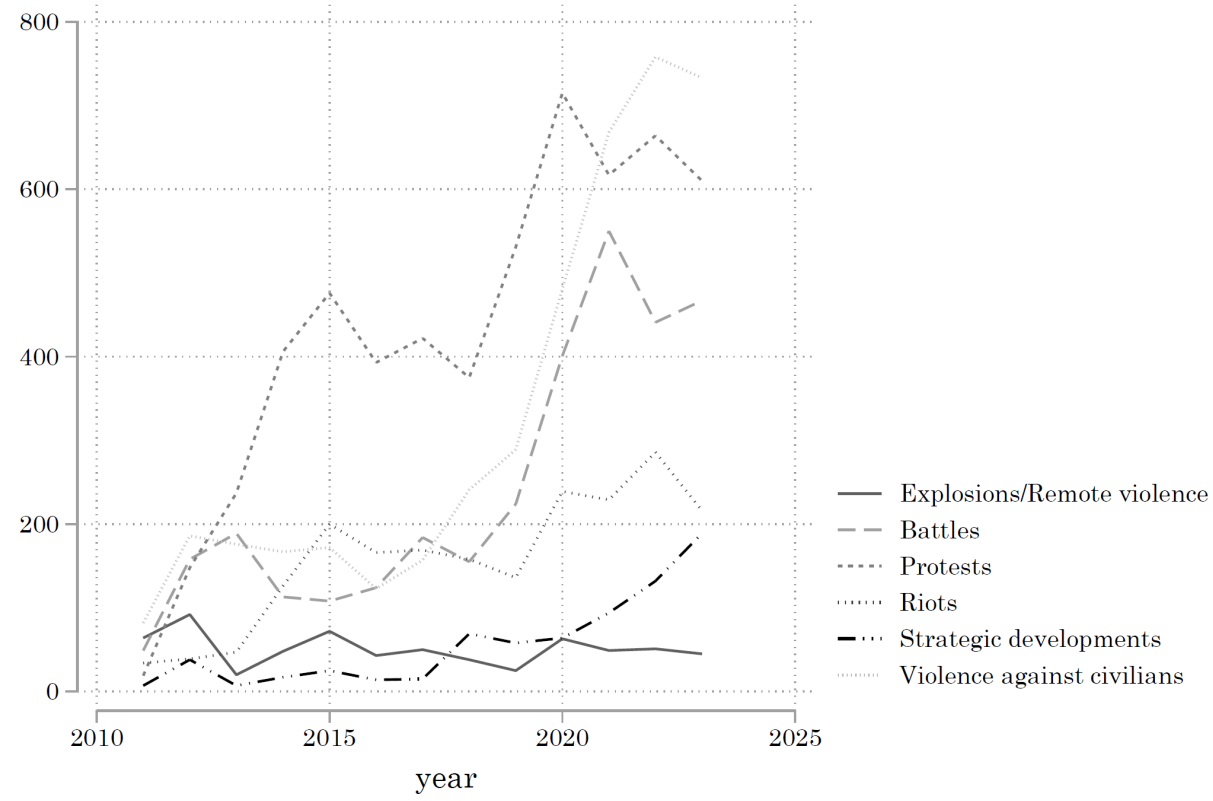

Source: ACLED data

Nonetheless, the spatial distribution is different in Nigeria compared to Mozambique, we surprisingly observe that a peak of conflicts number also occurs from 2018. However, three main types of conflicts occurred from 2018: battles, protests and violence against civilians. To capture the indirect effects of these conflicts and considering the uniform distribution of those conflicts in Nigeria, we implement a buffer zone surrounding each event. Four studies examining geographic accessibility to markets, health care, and education by rural households in West Africa inform our understanding of the average distances of these households to such amenities in Nigeria. They showed that rural households are generally within 5 to 7 kilometers of essential amenities like markets, health care, and schools. These distances ranged from 4.82 to 7.10 kilometers for health care and approximately 6.9 kilometers for schools.[14] In peri-urban areas, households are closer, typically within 1 to 2 kilometers of amenities, with distances ranging from 1 to 1.8 kilometers for primary schools and around 1 kilometer for secondary schools.[15] To represent the extent of the impact of conflicts depending on the degree of urbanization, we consider two types of buffers around each conflict: large and small (see figures 13 and 14). Figure 14 also shows evidence of the uniform spatial distribution of conflicts within Nigeria. As opposed to Mozambique, where we observed a concentrated spatial distribution of conflicts as well as the context in Nigeria regarding conflicts, we cannot derive the same buffer zone size. Regarding these differences in settlement between Mozambique and Nigeria, we decide to specify different buffer zone areas that should better reflect Nigeria's conflicts and population settlement (see Table 11).

[14] Adetunji (2020) found that rural traders in Nigeria lived an average of 6.56 kilometers from markets, while Tanou et al. (2021) reported distances of 5.29 to 7.10 kilometers to health care facilities in rural North Benin. Oldenburg et al. (2021) found that households with young children in Northwest Burkina Faso were approximately 4.82 kilometers from health care facilities. Popoola's (2022) research in Nigeria showed that rural villages were, on average, 6.9 kilometers from the nearest primary school.

Adetunji, Musilimu A. (2020). Households Travel Behaviour to Markets in Rural Communities in Ayedaade Local Government Area of Osun State, Nigeria. Journal of Asian Rural Studies, 4, 202. https://doi.org/10.20956/jars.v4i2.2336

Tanou, M., Kishida, T., & Kamiya, Y. (2021). The effects of geographical accessibility to health facilities on antenatal care and delivery services utilization in Benin: A cross-sectional study. Reproductive Health, 18(205). https://doi.org/10.1186/s12978-021-01249-x

Oldenburg, C. E., Sié, A., Ouattara, M., Bountogo, M., Boudo, V., Kouanda, I., Lebas, E., Brogdon, J. M., Lin, Y., Nyatigo, F., Arnold, B. F., & Lietman, T. M. (2021). Distance to primary care facilities and healthcare utilization for preschool children in rural northwestern Burkina Faso: Results from a surveillance cohort. BMC Health Services Research, 21(1), 212. https://doi.org/10.1186/s12913-021-06226-5

[15] In peri-urban areas, households are typically closer to amenities, with distances ranging from 1 to 2 kilometers. Popoola (2002) observed that households in peri-urban settlements near secondary towns or capital cities were around 1.2 to 1.8 kilometers from primary schools, and approximately 1 kilometer from secondary schools.

Popoola, A., Magidimisha-Chipungu, H., & Chipungu, L. (2022). Towards rural inclusion: Improving the governance of service delivery in Nigeria. Cogent Social Sciences, 8(1), 2118793. https://doi.org/10.1080/23311886.2022.2118793

Table 11. Buffer size by settlement type

		Settlement type		
		Urban	Suburban	rural
Buffer size	Large	1km	2km	10km
	Small	0.5km	1km	5km

Figure 13. Flood pixels and small conflict buffers in Nigeria

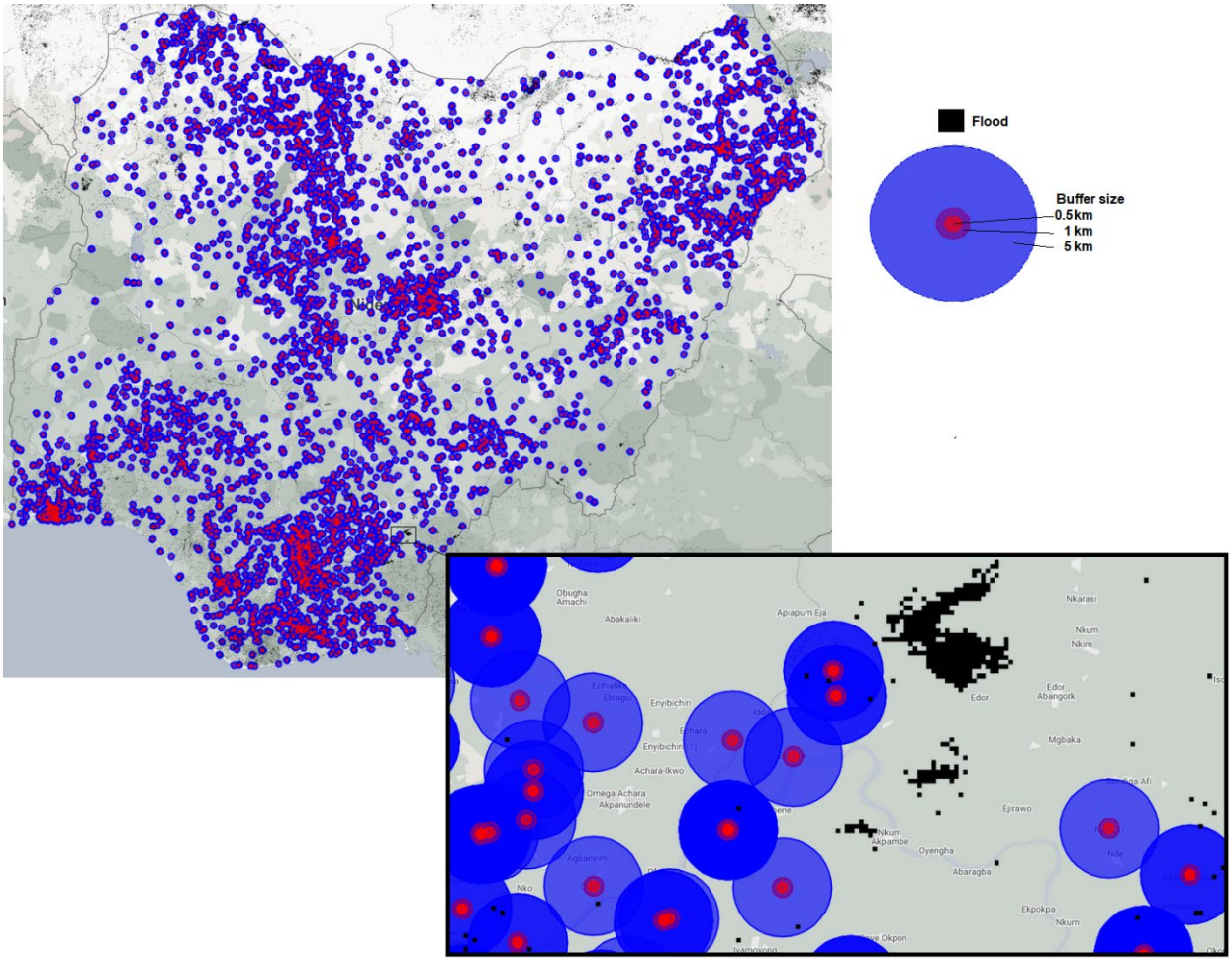

Note: the conflict categories depicted in this graph and used in the subsequent analysis are restricted to 'Battles', 'Explosions/Remote violence', and 'Violence against civilians'

Figure 14. Flood pixels and large conflict buffers in Nigeria

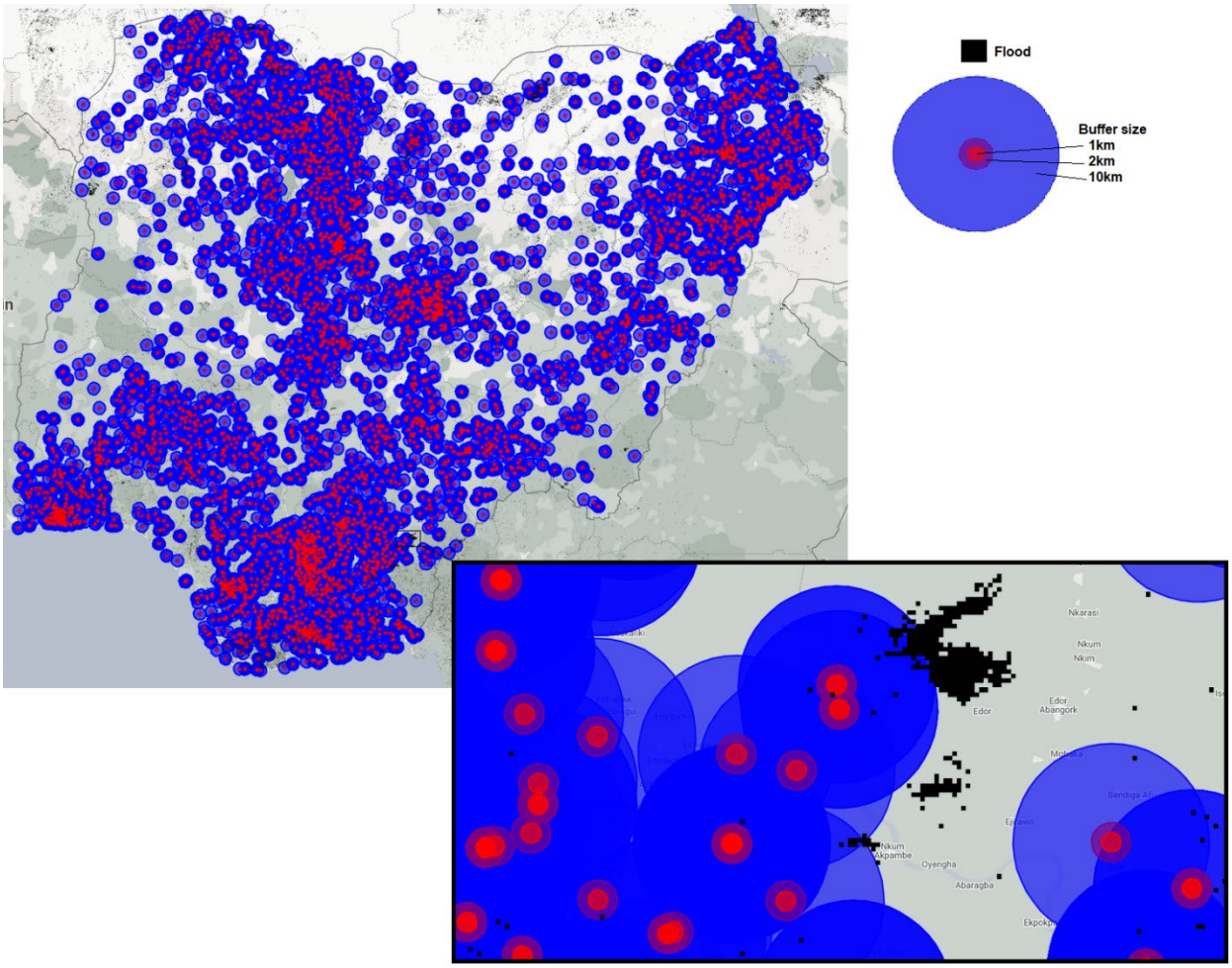

Note: the conflict categories depicted in this graph and used in the subsequent analysis are restricted to 'Battles', 'Explosions/Remote violence', and 'Violence against civilians'

Results : Nigeria

The results from the difference-in-difference regression support the observations made from inspecting the time series. The first column in Table 12 show the estimation results from equation (1) when considering small buffers around conflicts. The dependent variable is avg_radBuff05 and the period of interest is one month before the flood compared to one month after. The variable *Treated*PostPeriod,* which estimates the differentiated impact of the floods on nightlight radiance between conflict and non-conflict pixels, is negative and significant. This result shows that the flood led to a decline in nightlight radiance in 1.2% larger than in non-conflict-affected areas. The second column includes the additional covariate *cf_cvgBuff05*, which is the number of cloud-free images that were used in computing the average monthly radiance. Reassuringly, the effect is not significant. When including the *Urban_Suburban* dummy variable, the coefficient is positive and significant, indicating that nightlight radiance is than in urban and suburban areas than in rural settings (see column (3)). The *Fatalities* coefficient is also significant, but negative, showing that the larger the casualties of the conflict, the smaller the nightlight radiance.

Figure 15. Time series of mean nightlight (avg_radBuff05) for July floods in Nigeria using large conflict buffers

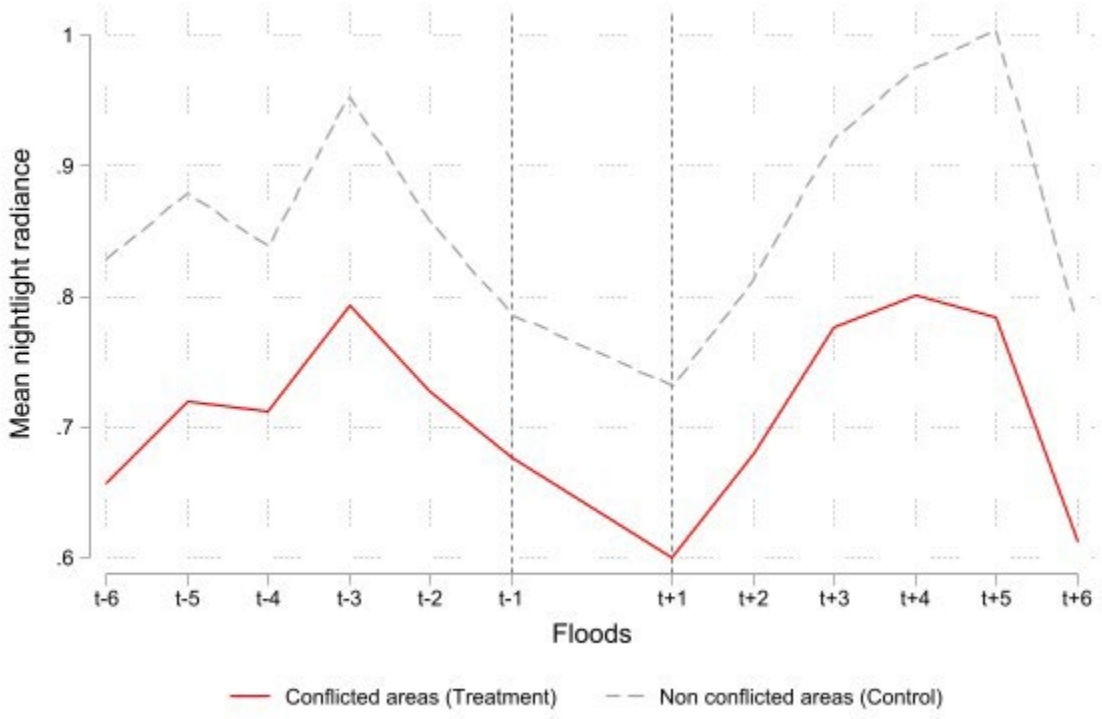

Note: The peak at t-3 (April 2022) can be explained by the event in which the federal government ordered the reopening of four international land borders (Idiroko border in Ogun State, Jibiya in Katsina, Kamba in Kebbi and Ikom border in Cross River), which had been closed since 2018 to prevent rice smuggling (IMF 2022, 26)

Table 12. Regression results for Nigeria for July floods in Nigeria and large conflict buffers

	(1)	(2)	(3)	(4)
	T-1 to t+1	T-1 to t+1	T-1 to t+1	T-1 to t+1
VARIABLES	avg_radBuff05	avg_radBuff05	avg_radBuff05	avg_radBuff05
Treated	-0.0522***	-0.0522***	-0.000604	0.000655
	(0.0109)	(0.0109)	(0.0105)	(0.0104)
PostPeriod	-0.0322***	-0.0392***	-0.0322***	-0.0322***
	(0.00488)	(0.00784)	(0.00488)	(0.00488)
Treated*PostPeriod	-0.0120**	-0.0119**	-0.0120**	-0.0120**
	(0.00547)	(0.00554)	(0.00547)	(0.00547)
PopDens	0.000505***	0.000505***	0.000408***	0.000413***
	(8.49e-05)	(8.48e-05)	(7.93e-05)	(7.95e-05)
cf_cvgBuff05		0.00148		
		(0.00132)		
Urban_Suburban			0.112***	0.112***
			(0.0156)	(0.0157)
Fatalities				-3.88e-05*
				(2.16e-05)
Constant	0.439***	0.433***	0.382***	0.382***
	(0.00633)	(0.00832)	(0.00826)	(0.00821)
Observations	13,330	13,330	13,330	13,330
R-squared	0.674	0.674	0.682	0.682
Treatment Obs	5342	5342	5342	5342
Control Obs	7988	7988	7988	7988

Notes: Robust standard errors in parentheses; *** p<0.01, ** p<0.05, * p<0.1; avg_radBuff05 ranges from 0.14 to 16.64.

Table 13. Regression results for July floods in Nigeria and large conflict buffers at different periods post July floods

	(1)	(2)	(3)	(4)	(5)	(6)
	T-1 to t+1	T-1 to t+2	T-1 to t+3	T-1 to t+4	T-1 to t+5	T-1 to t+6
VARIABLES	avg_radBuff05	avg_radBuff05	avg_radBuff05	avg_radBuff05	avg_radBuff05	avg_radBuff05
Treated	-0.0522***	-0.0554***	-0.0553***	-0.0600***	-0.0564***	-0.0531***
	(0.0109)	(0.0113)	(0.0111)	(0.0119)	(0.0122)	(0.0117)
PostPeriod	-0.0322***	0.0163***	0.0705***	0.0633***	0.0533***	-0.0445***
	(0.00488)	(0.00593)	(0.00689)	(0.00841)	(0.0108)	(0.00963)
Treated*PostPeriod	-0.0120**	-0.00657	-0.00898	-0.0101	-0.0232**	-0.0204**
	(0.00547)	(0.00713)	(0.00680)	(0.00877)	(0.0107)	(0.00957)
PopDens	0.000505***	0.000485***	0.000555***	0.000580***	0.000634***	0.000602***
	(8.49e-05)	(8.18e-05)	(8.59e-05)	(9.22e-05)	(9.82e-05)	(9.32e-05)
Constant	0.439***	0.441***	0.438***	0.438***	0.434***	0.434***
	(0.00633)	(0.00630)	(0.00655)	(0.00705)	(0.00792)	(0.00752)

Observations	13,330	13,330	13,330	13,330	13,330	13,330
R-squared	0.674	0.669	0.683	0.682	0.678	0.678
Treatment Obs	5342	5342	5342	5342	5342	5342
Control Obs	7988	7988	7988	7988	7988	7988

Notes: Robust standard errors in parentheses; *** p<0.01, ** p<0.05, * p<0.1; avg_radBuff05 ranges from 0.14 to 16.64.

Considering the flooded pixels whose values are available for the duration of the analysis, i.e., 6 months before and 6 months after the July floods, we first inspect the trend in mean nightlight radiance. Figure 15 shows that both conflict-affected (represented by the red line), and non-conflict-affected (represent by the dashed grey line) pixels follow a similar trajectory until the occurrence of the floods in July. Between t-1 (June 2022) and t+1 (August 2022), nightlight radiance and picks up again afterward, suggesting a temporary power outage due to the flood. However, the decline in radiance is sharper for conflicted areas than non-conflict affected areas. Furthermore, nightlight radiance in the conflict affected area rises more slowly than in the non-conflict area until December 2020, suggesting longer term structural differences between the two groups following the flooding event.

Robustness checks

To confirm the validity of our results, we proceed to apply a statistical robustness check for the common trend. The test consists of re-estimating the difference in difference regressions considering months prior to the flood event of July. The results presented in Table 14 show that the *Treated*PostPeriod* variable alternate between negative and positive values and is not significant and, confirming the common trend assumption is respected.

Table 14. Regression results for July floods in Nigeria and large conflict buffers testing common trends using log(nightlights), 1 to 6 months before the floods

VARIABLES	(1) t-2 to t-1 avg_radBuff05	(2) T-3 to t-2 avg_radBuff05	(3) T-4 to t-3 avg_radBuff05	(4) T-5 to t-4 avg_radBuff05	(5) T-6 to t-5 avg_radBuff05
Treated	-0.0597***	-0.0575***	-0.0579***	-0.0677***	-0.0733***
	(0.0108)	(0.0120)	(0.0120)	(0.0132)	(0.0137)
PostPeriod	-0.0493***	-0.0225***	0.0524***	-0.000375	0.0389***
	(0.00454)	(0.00633)	(0.00625)	(0.00726)	(0.00377)
Treated*PostPeriod	0.00693	-0.000900	-0.00428	0.00614	0.00676
	(0.00468)	(0.00651)	(0.00669)	(0.00729)	(0.00488)
PopDens	0.000507***	0.000554***	0.000568***	0.000606***	0.000697***
	(8.21e-05)	(8.77e-05)	(9.17e-05)	(9.92e-05)	(0.000112)
Constant	0.488***	0.508***	0.457***	0.457***	0.413***
	(0.00609)	(0.00685)	(0.00660)	(0.00787)	(0.00771)
Observations	13,330	13,330	13,330	13,330	13,330
R-squared	0.679	0.682	0.682	0.679	0.681
Treatment Obs	5342	5342	5342	5342	5342
Control Obs	7988	7988	7988	7988	7988

Notes: Robust standard errors in parentheses; *** p<0.01, ** p<0.05, * p<0.1; avg_radBuff05 ranges from 0.14 to 16.64.

Limitation and Discussion

Assessing the quantitative impact of disasters on populations and economies is particularly challenging in poor and conflict-affected regions, where reliable socio-economic data may be lacking. Our analysis of descriptive statistics has indicated a tendency towards lower nightlight density in rural areas, which could potentially lead to an underestimation of economic activity due to the limitations in spatial resolution. Nightlight radiance in rural settings is typically less intense than in urban centers, and a higher incidence of such readings could result in a skewed sample. Furthermore, sectors like agriculture, which are less dependent on electricity, might not be fully represented by nightlight data. This is particularly true for poorer households in rural areas that may not have access to electricity, rendering them invisible in satellite-based observations. Consequently, vital aspects of a developing economy might be missed when relying exclusively on nightlight data for analysis.

Nonetheless, and despite these limitations, access to advanced earth observation technologies, including regularly updated satellite imagery, presents new avenues for analysis using quasi-experimental approaches. Nightlight satellite data can provide valuable insights into economic activity, primarily enabling the assessment of immediate to short-term impacts. Our case studies highlight the exacerbated effects of floods on nightlight in conflict-affected regions. For instance, we observed a decrease in nightlight radiance following the July 2022 floods in Nigeria, with conflict-

affected areas experiencing up to 1.2% greater negative impacts than non-conflict areas. Similar patterns were observed in Mozambique, where cyclones led to a 1.39% reduction in economic activities in conflict-affected populations compared to their non-conflict-affected counterparts. As a potential next step, a long-term difference in difference regression analysis, as well as the use of observational data that could be more nuanced and contextual, could explore, in addition to the short-term impact identified here, the long-term impact of disasters dynamics in conflict settings.

To fully comprehend these dynamics, it is essential to conduct further research to pinpoint the causal factors that exacerbate vulnerability in conflict-stricken settings. Our findings, however, emphasize the critical need for investment in disaster risk reduction and the prioritization of recovery initiatives in conflict-affected regions. Inhabitants of these areas suffer more significant impacts and face extended recovery periods in the aftermath of disasters, underscoring the necessity for focused interventions to reduce their vulnerabilities and bolster their resilience.

Conclusion

While extensive research has examined the impacts of disasters on conflict dynamics, less attention has been given to understanding how conflicts influence disaster impacts and recovery. By employing a difference-in-difference method alongside geospatial and satellite imagery datasets, this paper seeks to address this literature gap by estimating the impacts of a disaster in conflict settings and contrasting them with impacts in non-conflict settings.

This study represents one of the initial attempts to quantitatively compare the diverging impacts of a disaster between conflict and non-conflict affected regions. Our findings suggest that in the aftermath of the floods of interest, conflict-affected areas in Nigeria and Mozambique experienced the most severe negative impacts following the flood event, up to 1.2% and 1.39%, respectively. These results indicate that conflict-affected areas bore a heavier burden of the floods compared to non-conflict areas. Additionally, the negative impacts in conflict settings continued to be larger than in non-conflict affected regions for the six months following the event, which gives an indication that these floods prolonged the recovery period for conflict-affected populations.

In conclusion, despite existing methodological constraints, our study demonstrates that the impacts of disasters are significantly more pronounced in conflict settings compared to non-conflict areas. In the next phase of our analysis, we aim to supplement the current 'top-down' approach of assessing disaster impacts through satellite imagery with a 'bottom-up' approach using panel household survey data. By combining both approaches, we will gain insights into household-level impacts and their variations between conflict and non-conflict areas.

References

ACLED. (2023). *ACLED | Bringing Clarity to Crisis*. https://acleddata.com/

Bertinelli, L., & Strobl, E. (2013). Quantifying the Local Economic Growth Impact of Hurricane Strikes. *Journal of Applied Meteorology and Climatology*, *52*(8). https://doi.org/https://doi.org/10.1175/JAMC-D-12-0258.1

Bickenbach, F., Bode, E., Nunnenkamp, P., & Söder, M. (2016). Night lights and regional GDP. *Review of World Economics*, *152*(2), 425–447. https://doi.org/10.1007/S10290-016-0246-0/TABLES/12

Brzoska, M. (2018). Weather Extremes, Disasters, and Collective Violence: Conditions, Mechanisms, and Disaster-Related Policies in Recent Research. *Current Climate Change Reports*, 4(4), 320–329. https://doi.org/10.1007/s40641-018-0117-y

Card, D., & Krueger, A. B. (2000). Minimum Wages and Employment: A Case Study of the Fast-Food Industry in New Jersey and Pennsylvania: Reply. *American Economic Review*, *90*(5), 1397–1420. https://doi.org/10.1257/AER.90.5.1397

Chen, X., & Nordhaus, W. D. (2011). Using luminosity data as a proxy for economic statistics. *Proceedings of the National Academy of Sciences of the United States of America*, *108*(21), 8589–8594. https://doi.org/10.1073/PNAS.1017031108/SUPPL_FILE/SAPP.PDF

DeVries, B., Huang, C., Armston, J., Huang, W., Jones, J. W., & Lang, M. W. (2020). Rapid and robust monitoring of flood events using Sentinel-1 and Landsat data on the Google Earth Engine. *Remote Sensing of Environment*, *240*. https://doi.org/10.1016/J.RSE.2020.111664

Echendu, A. J. (2020). The impact of flooding on Nigeria's sustainable development goals (SDGs). *Ecosystem Health and Sustainability*, *6*(1). https://doi.org/10.1080/20964129.2020.1791735

Elliott, R. J. R., Strobl, E., & Sun, P. (2015). The local impact of typhoons on economic activity in China: A view from outer space. *Journal of Urban Economics*, *88*, 50–66. https://doi.org/10.1016/J.JUE.2015.05.001

Elvidge, C. D., Baugh, K., Zhizhin, M., Hsu, F. C., & Ghosh, T. (2017). VIIRS night-time lights. *International Journal of Remote Sensing*, *38*(21), 5860–5879. https://doi.org/10.1080/01431161.2017.1342050

EM-DAT, & CRED / UCLouvain. (2023). *The international Disaster Database*. www.emdat.be

ESA. (2023). *Sentinel-1*. Https://Sentinels.Copernicus.Eu/Web/Sentinel/Copernicus/Sentinel-1.

Facebook Connectivity Lab and Center for International Earth Science Information Network - CIESIN - Columbia University. (2016). *High Resolution Settlement Layer (HRSL)*. Source Imagery for HRSL © 2016 DigitalGlobe. https://data.humdata.org/dataset/highresolutionpopulationdensitymaps

Felbermayr, G., Gröschl, J., Sanders, M., Schippers, V., & Steinwachs, T. (2022). The economic impact of weather anomalies. *World Development*, *151*, 105745. https://doi.org/10.1016/J.WORLDDEV.2021.105745

Galiani, S., Gertler, P., & Schargrodsky, E. (2005). Water for life: The impact of the privatization of water services on child mortality. *Journal of Political Economy*, *113*(1), 83–120. https://doi.org/10.1086/426041

Gemenne, F., Barnett, J., Adger, W. N., & Dabelko, G. D. (2014). Climate and security: Evidence, emerging

risks, and a new agenda. *Climatic Change*, *123*(1), 1–9. https://doi.org/10.1007/S10584-014-1074-7/METRICS

Ghimire, R., Ferreira, S., & Dorfman, J. H. (2015). Flood-Induced Displacement and Civil Conflict. *World Development*, 66, 614–628. https://doi.org/10.1016/j.worlddev.2014.09.021

Gibson, J., Olivia, S., Boe-Gibson, G., & Li, C. (2021). Which night lights data should we use in economics, and where? *Journal of Development Economics*, *149*, 102602. https://doi.org/10.1016/J.JDEVECO.2020.102602

Gillespie, T. W., Frankenberg, E., Chum, K. F., & Thomas, D. (2014). Nighttime lights time series of tsunami damage, recovery, and economic metrics in Sumatra, Indonesia. *Remote Sensing Letters (Print)*, *5*(3), 286. https://doi.org/10.1080/2150704X.2014.900205

Gilmore, E. A. (2017). Introduction to Special Issue: Disciplinary Perspectives on Climate Change and Conflict. *Current Climate Change Reports*, *3*(4), 193–199. https://doi.org/10.1007/S40641-017-0081-Y/TABLES/1

Gleditsch, N. P. (2012). Whither the weather? Climate change and conflict. *Journal of Peace Research*, *49*(1), 3–9. https://doi.org/https://doi.org/10.1177/002234331143128

Hallegatte, S., Vogt-Schilb, A., Bangalore, M., & Rozenberg, J. (2017). Unbreakable: Building the Resilience of the Poor in the Face of Natural Disasters. *Unbreakable: Building the Resilience of the Poor in the Face of Natural Disasters*. https://doi.org/10.1596/978-1-4648-1003-9

Heger, M. P., & Neumayer, E. (2019). The impact of the Indian Ocean tsunami on Aceh's long-term economic growth. *Journal of Development Economics*, *141*, 102365. https://doi.org/10.1016/J.JDEVECO.2019.06.008

Henderson, J. V., Storeygard, A., & Weil, D. N. (2012). Measuring Economic Growth from Outer Space. *American Economic Review*, *102*(2), 994–1028. https://doi.org/10.1257/AER.102.2.994

IMF (2023). Nigeria: 2022 Article IV Consultation -- Press Release; Staff Report; Staff Statement; and Statement by the Executive Director for Nigeria. IMF Country report No. 23/93.

Kocornik-Mina, A., McDermott, T. K. J., Michaels, G., & Rauch, F. (2020). Flooded Cities. *American Economic Journal: Applied Economics*, *12*(2), 35–66. https://doi.org/10.1257/APP.20170066

Linard, C., Gilbert, M., Snow, R. W., Noor, A. M., & Tatem, A. J. (2012). Population Distribution, Settlement Patterns and Accessibility across Africa in 2010. *PLOS ONE*, *7*(2), e31743. https://doi.org/10.1371/JOURNAL.PONE.0031743

Miranda Montero, J. J., Ishizawa Escudero, O. A., & Strobl, E. (2017). *The impact of hurricane strikes on short-term local economic : evidence from nightlight images in the Dominican Republic*. World Bank Group.

Nardulli, P. F., Peyton, B., & Bajjalieh, J. (2015). Climate Change and Civil Unrest: The Impact of Rapid-onset Disasters. *Journal of Conflict Resolution*, 59(2), 310-335. https://doi.org/10.1177/0022002713503809

Nel, P., & Righarts, M. (2008). Natural Disasters and the Risk of Violent Civil Conflict. International Studies Quarterly, 52(1), 159–185. https://doi.org/10.1111/j.1468-2478.2007.00495.x

Nordås, R., & Gleditsch, N. P. (2007). Climate change and conflict. *Political Geography*, *26*(6), 627–638.

https://doi.org/10.1016/J.POLGEO.2007.06.003

Odozi, J. C., & Oyelere, R. U. (2022). *Violent Conflict Exposure in Nigeria and Household Welfare: What Can We Learn from Panel Data?* Allied Social Science Associations (ASSA) Annual Meeting.

Pekel, J. F., Cottam, A., Gorelick, N., & Belward, A. S. (2016). High-resolution mapping of global surface water and its long-term changes. *Nature 2016 540:7633*, *540*(7633), 418–422. https://doi.org/10.1038/nature20584

Peters, K., Holloway, K., & Peters, L. E. R. (2019). Disaster risk reduction in conflict contexts: The state of the evidence [Working paper]. *Overseas Development Institute*. https://apo.org.au/node/235271

Salehyan, I. (2014). Climate change and conflict: Making sense of disparate findings. *Political Geography*, *43*, 1–5. https://doi.org/10.1016/J.POLGEO.2014.10.004

Schiavina, M., Melchiorri, M., & Pesaresi, M. (2023). *GHS-SMOD R2023A - GHS settlement layers, application of the Degree of Urbanisation methodology (stage I) to GHS-POP R2023A and GHS-BUILT-S R2023A, multitemporal (1975-2030)*. European Commission, Joint Research Centre (JRC). https://data.jrc.ec.europa.eu/dataset/a0df7a6f-49de-46ea-9bde-563437a6e2ba

Schippers, V., & Botzen, W. (2023). Uncovering the veil of night light changes in times of catastrophe. *Natural Hazards and Earth System Sciences*, *23*(1), 179–204. https://doi.org/10.5194/NHESS-23-179-2023

Schleussner, C.-F., Donges, J. F., Donner, R. V., & Schellnhuber, H. J. (2016). Armed-conflict risks enhanced by climate-related disasters in ethnically fractionalized countries. *Proceedings of the National Academy of Sciences*, 113(33), 9216–9221. https://doi.org/10.1073/pnas.1601611113

Selby, J., & Hoffmann, C. (2014). Rethinking Climate Change, Conflict and Security. *Geopolitics*, *19*(4), 747–756. https://doi.org/10.1080/14650045.2014.964866

Slettebak, R. T. (2012). Don't blame the weather! Climate-related natural disasters and civil conflict. *Journal of Peace Research*, 49(1), 163-176. https://doi.org/10.1177/0022343311425693

Siddiqi, A. (2018). Disasters in conflict areas: finding the politics. *Disasters*, *42*, S161–S172. https://doi.org/10.1111/DISA.12302

Skoufias, E., Strobl, E., & Tveit, T. (2021). Can we rely on VIIRS nightlights to estimate the short-term impacts of natural hazards? Evidence from five South East Asian countries. *Geomatics, Natural Hazards and Risk*, *12*(1), 381–404. https://doi.org/10.1080/19475705.2021.1879943

Victor, N. U. (2021). Environmental Impact of Flooding on Rural Development in Southeastern Nigeria. *Journal of Environmental Hazards*, *5*(5).

WorldPop.org. (2024). *WorldPop Global Project Population Data*. www.worldpop.org

World Bank. (2004). *Classification of Fragility and Conflict Situations (FCS) for World Bank Group Engagement*, 1

World Bank. (2016). *Disaster recovery in conflict contexts: thematic case study for the disaster recovery framework guide (English).* Washington, D.C.: World Bank Group. http://documents.worldbank.org/curated/en/310171495026430229/Disaster-recovery-in-conflict-contexts-thematic-case-study-for-the-disaster-recovery-framework-guide

Appendix 1: Mozambique – different buffer sizes

To confirm that the choice of buffer area around conflicts does not impact our results, we further re-estimate our preferred specification at different buffer sizes, ranging from 100km to 10km around conflicts. As shown in Table 15, the difference-in-difference impacts remain significant and of similar magnitude for all buffer sizes, until 30km. When considering a small area around conflict, the impact becomes insignificant and the number of observations for the treatment group decreases considerably. Those results support the preferred buffer size of 60km.

Table 15. Regression results for conflicts within different buffers, preferred specification, 1 month post TCs

VARIABLES	(1) Period -1 to 1 Buffer 100km	(2) Period -1 to 1 Buffer 90km	(3) Period -1 to 1 Buffer 80km	(4) Period -1 to 1 Buffer 70km	(5) Period -1 to 1 Buffer 60km	(6) Period -1 to 1 Buffer 50km	(7) Period -1 to 1 Buffer 40km	(8) Period -1 to 1 Buffer 30km	(9) Period -1 to 1 Buffer 20km	(10) Period -1 to 1 Buffer 10km
Treated	0.00291	0.0104*	0.0114**	0.0120***	0.0136***	0.0150**	0.0212*	0.0456***	0.0514**	0.0883**
	(0.00961)	(0.00561)	(0.00484)	(0.00389)	(0.00510)	(0.00731)	(0.0110)	(0.0145)	(0.0217)	(0.0372)
PostPeriod	-0.0343***	-0.0335***	-0.0353***	-0.0369***	-0.0370***	-0.0375***	-0.0378***	-0.0395***	-0.0423***	-0.0430***
	(0.00487)	(0.00488)	(0.00484)	(0.00448)	(0.00437)	(0.00441)	(0.00420)	(0.00380)	(0.00377)	(0.00355)
*Treated*PostPeriod*	-0.0116**	-0.0137**	-0.0133**	-0.0121**	-0.0139**	-0.0140**	-0.0130*	-0.0125*	0.000103	0.00953
	(0.00570)	(0.00611)	(0.00651)	(0.00575)	(0.00555)	(0.00602)	(0.00683)	(0.00687)	(0.00686)	(0.00806)
PopDens	0.00234***	0.00236***	0.00248***	0.00241***	0.00244***	0.00243***	0.00234***	0.00259***	0.00256***	0.00253***
	(0.000549)	(0.000551)	(0.000563)	(0.000578)	(0.000575)	(0.000569)	(0.000532)	(0.000436)	(0.000438)	(0.000457)
urban	0.163***	0.163***	0.169***	0.172***	0.170***	0.170***	0.171***	0.161***	0.158***	0.154***
	(0.0352)	(0.0353)	(0.0354)	(0.0362)	(0.0354)	(0.0348)	(0.0340)	(0.0323)	(0.0317)	(0.0296)
Constant	0.160***	0.154***	0.154***	0.154***	0.155***	0.155***	0.155***	0.151***	0.155***	0.157***
	(0.00875)	(0.00487)	(0.00425)	(0.00389)	(0.00468)	(0.00520)	(0.00530)	(0.00458)	(0.00405)	(0.00353)
Observations	17,884	18,078	18,396	18,476	18,698	18,770	19,006	19,602	20,424	21,362
Treatment Obs	15,496	13,940	12,670	11,198	8,920	7,462	5,674	4,202	2,470	1,024
Control Obs	2,388	4,138	5,726	7,278	9,778	11,308	13,332	15,400	17,954	20,338
R-squared	0.470	0.468	0.480	0.474	0.478	0.483	0.486	0.504	0.500	0.485

Notes: Robust standard errors in parentheses; *** p<0.01, ** p<0.05, * p<0.1; avg_radBuff05 range from .06 to 3.7.

Appendix 2: Tables and figures for the Nigeria case study

Table 6. Variables description for additional variables

Variable	Description	Unit
pop_WorldPop_dens_km2	WorldPop Population density	Person/km^2
cf_cvg	Total number of cloud-free observations that went into each pixel	
avg_rad	Average Nightlight radiance values	nanoWatts/sr/cm^2

Table 7. Summary statistics for habited flooded pixels (rural, suburban and urban categories) sample for large conflict buffers

__	N	Mean	SD	Min	p5	Median	p95	Max
cf_cvgBuff05	114,289	8.13	4.16	1	1.83	8.19	14	23.63
cf_cvg	114,289	8.13	4.17	1	2	8	14	24
avg_radBuff05	114,289	1.43	13.99	0.02	0.19	0.37	3.95	1,553.18
avg_rad	114,289	1.42	17.37	0.01	0.18	0.37	3.9	2,363.48
nb_conflict	114,289	4.11	14.24	0	0	0	18	625
Treated	114,289	0.39	0.49	0	0	0	1	1
Treated_after	114,289	0.22	0.41	0	0	0	1	1
Fatalities	114,289	19.5	137.75	0	0	0	49	4450
settlement	114,289	15.67	4.87	12	12	12	23	23
Urban_Suburban	114,289	0.37	0.48	0	0	0	1	1

Table 8. Summary statistics for habited flooded pixels (rural, suburban and urban categories) sample for small conflict buffers

	N	Mean	SD	Min	p5	Median	p95	Max
cf_cvgBuff05	114,289	8.13	4.16	1	1.83	8.19	14	23.63
cf_cvg	114,289	8.13	4.17	1	2	8	14	24
avg_radBuff05	114,289	1.43	13.99	0.02	0.19	0.37	3.95	1,553.18
avg_rad	114,289	1.42	17.37	0.01	0.18	0.37	3.9	2,363.48
nb_conflict	114,289	0.88	4.82	0	0	0	4	192
Treated	114,289	0.15	0.36	0	0	0	1	1
Treated_after	114,289	0.08	0.27	0	0	0	1	1
Fatalities	114,289	4.37	60.23	0	0	0	8	2464
settlement	114,289	15.67	4.87	12	12	12	23	23
Urban_Suburban	114,289	0.37	0.48	0	0	0	1	1

Figure 16. Mean avg_rad and avg_radBuff05 for all flooded grid cells over the analysis period

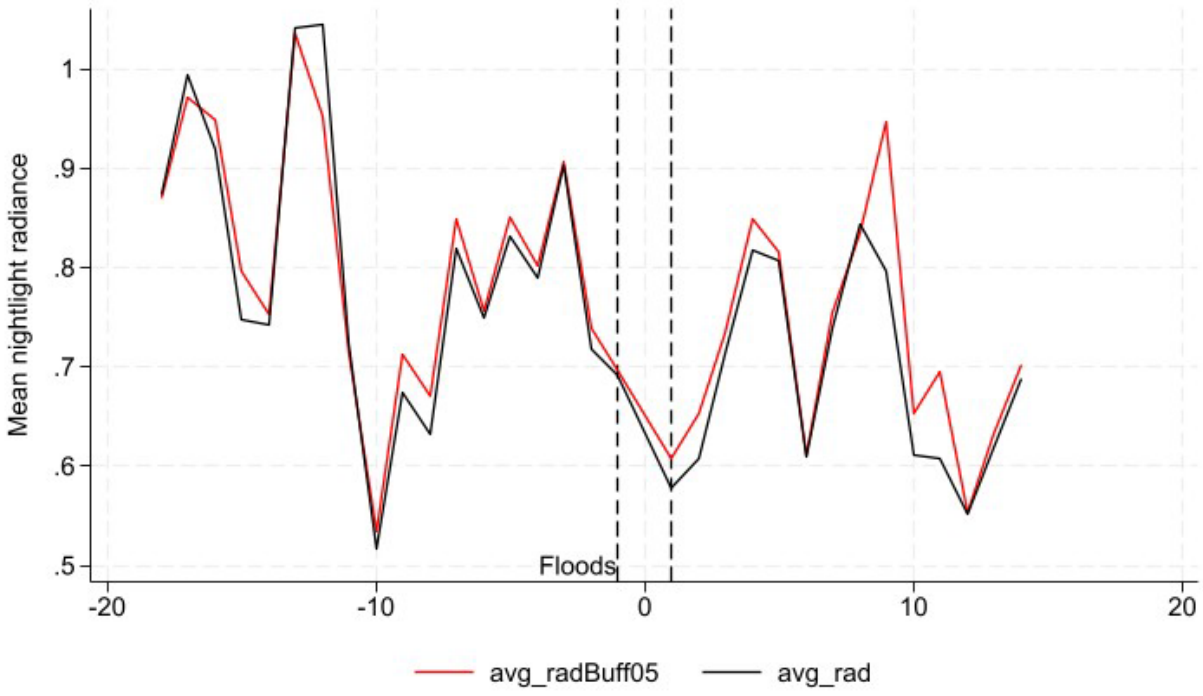

Figure 17. Mean cf_cvg and cf_cvgBuff05 for all flooded grid cells over the analysis period

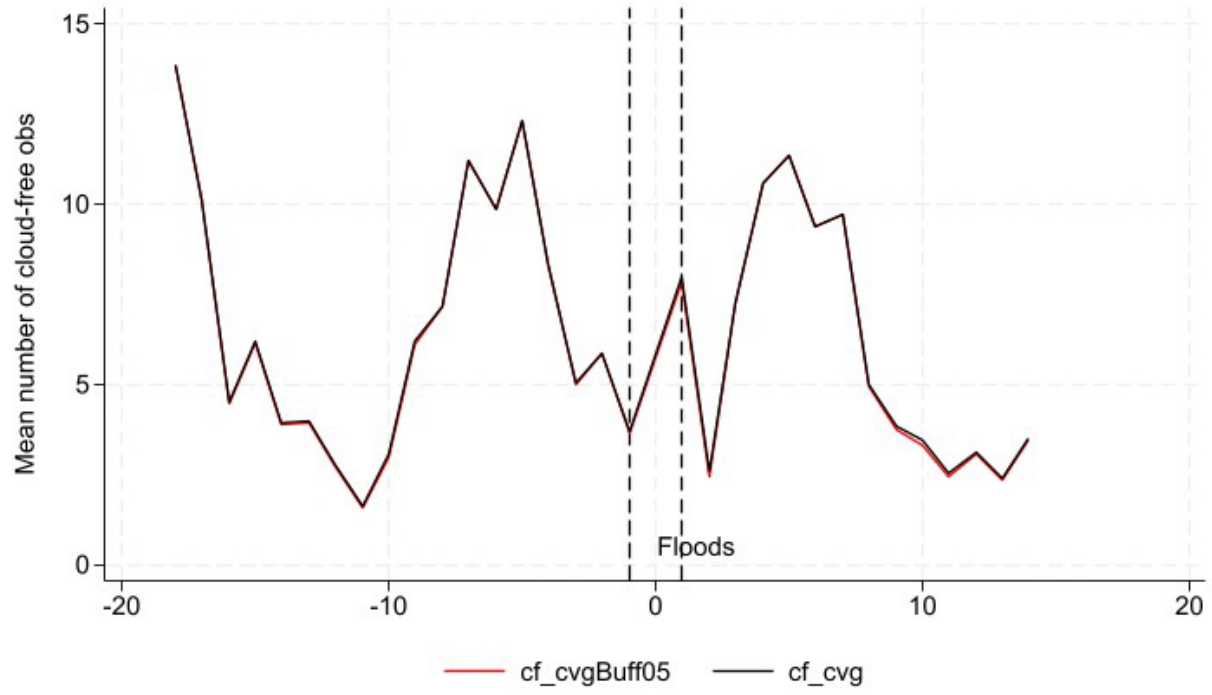

Table 16. Regression results of equation (1) using alternative population variables for 1 month post July floods. Dependent variable avg_radBuff05

	(1)	(2)
	T-1 to t+1	T-1 to t+1
VARIABLES	avg_radBuff05	avg_radBuff05
Treated	-0.0522***	-0.0379***
	(0.0109)	(0.00953)
PostPeriod	-0.0322***	-0.0322***
	(0.00488)	(0.00488)
Treated*PostPeriod	-0.0120**	-0.0120**
	(0.00547)	(0.00547)
PopDens	0.000505***	
	(8.49e-05)	
pop_WorldPop_dens_km2		0.00251***
		(0.000215)
Constant	0.439***	0.361***
	(0.00633)	(0.00883)
Observations	13,330	13,330
R-squared	0.674	0.718
Treatment Obs	5342	5342
Control Obs	7988	7988

Notes: Robust standard errors in parentheses; *** p<0.01, ** p<0.05, * p<0.1; avg_radBuff05 ranges from .06 to 3.7

Table 0. Regression results for conflicts with different buffers and nightlight radiance variables, 1 month post July floods

	(1)	(2)	(3)	(4)
	T-1 to t+1	T-1 to t+1	T-1 to t+1	T-1 to t+1
buffer	large	small	large	small
VARIABLES	avg_radBuff05	avg_radBuff05	avg_rad	avg_rad
Treated	-0.0522***	-0.0413***	-0.0462***	-0.0322***
	(0.0109)	(0.0123)	(0.0110)	(0.0119)
PostPeriod	-0.0322***	-0.0346***	-0.0307***	-0.0320***
	(0.00488)	(0.00440)	(0.00477)	(0.00430)
Treated*PostPeriod	-0.0120**	-0.0123*	-0.0116**	-0.0184**
	(0.00547)	(0.00722)	(0.00592)	(0.00744)
PopDens	0.000505***	0.000507***	0.000525***	0.000523***
	(8.49e-05)	(8.53e-05)	(9.21e-05)	(9.22e-05)
Constant	0.439***	0.424***	0.423***	0.409***
	(0.00633)	(0.00519)	(0.00636)	(0.00524)
Observations	13,330	13,482	11,976	12,098
R-squared	0.674	0.670	0.677	0.675
Treatment Obs	5342	2096	4774	1844
Control Obs	7988	11386	7202	10254
Range of dependent variable	.06 to 3.7	0.14 to 16.64	0.12 to 16.53	0.13 to 16.53

Notes: Robust standard errors in parentheses; *** p<0.01, ** p<0.05, * p<0.1.

Figure 18. Time series for conflicts with different buffers and nightlight radiance variables for July floods in Nigeria
mean nightlight radiance

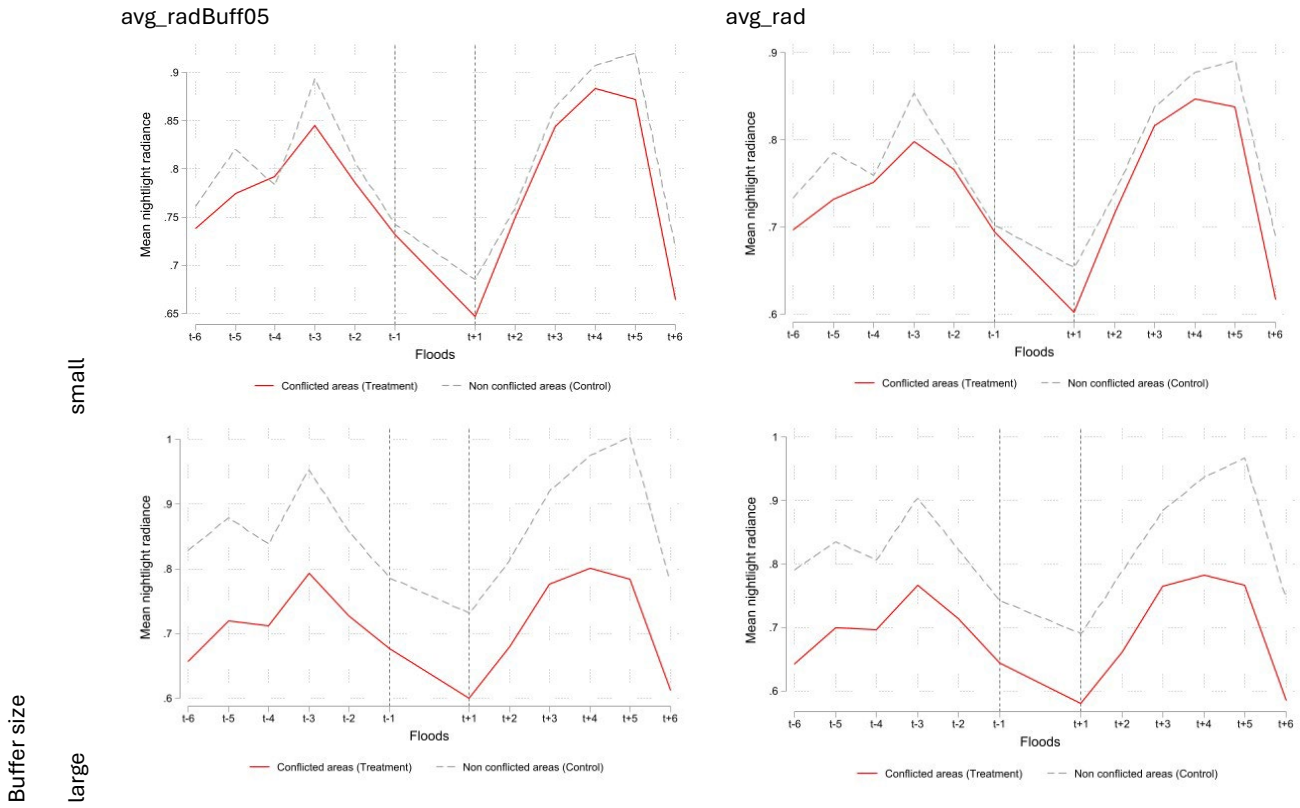

Table 1. Regression results of equation (1) using fixed effect model for 1 month post July floods. Dependent variable avg_radBuff05

	(1)
	T-1 to t+1
	Buffer large
VARIABLES	avg_radBuff05
o.Treated	-
PostPeriod	-0.0322***
	(0.00477)
Treated*PostPeriod	-0.0120**
	(0.00535)
o.PopDens	-

Constant	0.443***
	(0.00212)
Observations	13,330
R-squared	0.055
Number of ID_flooded	6,665
Treatment Obs	5342
Control Obs	7988

Notes: Robust standard errors in parentheses; *** p<0.01, ** p<0.05, * p<0.1; .14 to 16.64